2009

DESIGN AND EVALUATION OF PORTABLE PSYCHOACOUSTIC TESTING SYSTEMS

Qingyi Meng

DESIGN AND EVALUATION OF PORTABLE PSYCHOACOUSTIC TESTING SYSTEMS

(Spine title: Portable Psychoacoustic Testing Systems)

(Thesis format: Monograph)

by

Qingyi Meng

Graduate Program
in
Engineering Science
Department of Electrical and Computer Engineering

A thesis submitted in partial fulfillment
of the requirements for the degree of
Master of Engineering Science

The School of Graduate and Postdoctoral Studies
The University of Western Ontario
London, Ontario, Canada

Abstract

There is an increasing demand for developing portable psychoacoustic testing systems to evaluate the hearing abilities of people. In this thesis, the design, development, and evaluation of portable, flexible, and versatile wired and wireless psychoacoustic testing systems will be presented.

The design of the wired system utilizes a USB audio I/O controller chip for communicating with the application software on the host through a USB cable. The wireless system includes two units: a transmitter and a receiver. 2.4GHz RF transceiver chips are employed for wireless communication. Double-side PCBs populated with 0603 SMD were designed and fabricated. To go along with the hardware, software was developed on a handheld device to control and execute several psychoacoustic tests and to log subjective data. Objective measurements and small scale clinical trials were undertaken to test the efficiency of the proposed portable systems.

Keywords: Wireless; Firmware; Hardware; Evaluation; USB; MCU; nRF24Z1; Subjective measurement

Acknowledgement

First and foremost, I would like to express my gratitude to my advisor, Dr. Vijay Parsa for his expertise, guidance, and support throughout this entire process. He also developed the application software for these systems which provides professional and powerful functions.

I would like to thank Eugen Porter for his great help in PCB making and population. He also revised and re-laid out the PCBs after I finished the prototypes. He is so nice and very patient for any questions. And I would also like to thank all others of electronics-shop personnel in the Electrical and Computer Engineering Department for their support in this entire process.

I would like to express my deepest gratitude to Steve Beaulac. He developed USB driver and contributed much for this project. I am also thankful to Adam Love, for developing the first version application software.

I greatly appreciate the contribution from Matthew Hannan. He performed the subjective hearing measurement and provided the results for my thesis.

I would like to acknowledge the support of all colleges in DSP lab. They include Kareemunnisa Asma, Rob McDonald, and David Suelzle.

Finally, I would like to say thanks to my family, my wife and my daughter. I am able to sense them all day.

Table of Contents

List of Tables

List of Figures

Nomenclature

ADC	Analog-to-Digital Converter
DAC	Digital-to-Analog Converter
D/A	Digital-to-Analog Converter
Codec	Coder-decoder
db	Decibel
Ghz	Giga Hertz
IC	Integrated Circuit
HL	Hearing Level
MIPS	Million Instructions per Second
ISP	In-System Programming
RMS	Root Mean Square
SPL	Sound Pressure Level
USB	Universal Serial Bus
GUI	Graphical User Interface
SOF	Start of Frame
EP	Endpoint
SPI	Serial Peripheral Interface
PCB	Printed Circuit Board
B&K	Bruel & Kjaer
THD	Total Harmonic Distortion
HATS	Head and Torso Simulator
SMD	Surface Mount Device

MCU	Microcontroller
Tp	Period duration
FHSS	Frequency Hopping Spread Spectrum
GPIO	General Purpose IO
IRQ	Interrupt Request
FSM	Finite State Machine

Chapter 1

Introduction

1.1 Hearing and Hearing Loss

Hearing is the ability of human beings to detect sound. Figure 1-1 shows the structure of the human ear, which is divided into outer ear, middle ear and inner ear. Briefly speaking, when sound waves are funneled into the ear canal, they set the ear drum into vibration. These vibrations are mechanically transferred through a chain of bones in the middle ear to the inner ear. The inner ear contains a fluid filled organ called cochlea, which consists of tiny hair cells that generate electrical impulses in response to the vibrations. The impulses are carried to the brain through the auditory nerve where they are interpreted for their content.

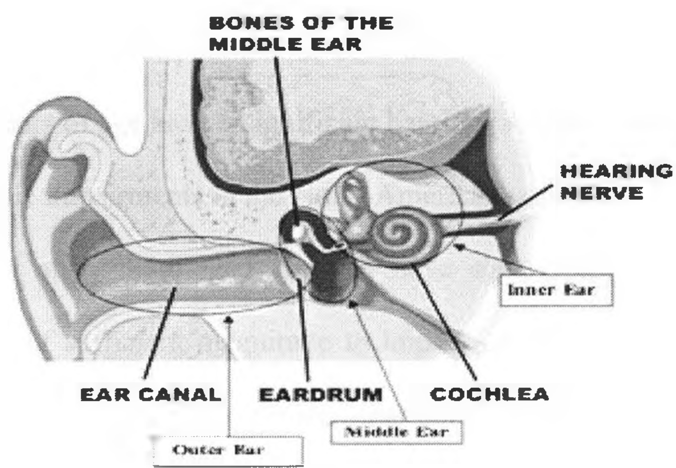

Figure 1-1: The Structure of the Ear [1]

A full or partial loss of the ability to detect and interpret sounds is called hearing impairment. Hearing impairment can either be peripheral hearing loss or central hearing loss. Peripheral hearing loss occurs due to abnormal functioning of the outer, middle, or inner ear structures. When the sound signals are not transduced properly by the outer or middle ear components, the hearing loss is termed as *conductive hearing loss* [1, 5]. The inability of the inner ear to transduce vibrations into nerve signals is termed as *sensorineural hearing loss* [2, 3].

In addition, there are conditions where significant auditory system damage or dysfunction may be present beyond the auditory periphery. Two auditory pathologies for example, Auditory Neuropathy/Dyssynchrony (AN/D) and Auditory Processing Disorders (APDs), have shown that significant impairment in hearing function (e.g., poor understanding of speech in diverse acoustic environments) can be present even in the presence of normal peripheral auditory functioning [3,4].

Hearing loss is the third most common ailment after arthritis and hypertension [1]. Approximately 10% of the general population, 20% of those over 65 years of age and 40% of those over 75 years of age have a significant hearing problem, making this one of the most common chronic impairments in the North American population [2]. In addition, 8 to 10% of preschool and school-aged children have some form of permanent or fluctuating hearing loss of sufficient magnitude to impact on their communication and language learning skills [2]. It is also estimated that about 5% of children suffer from central auditory processing disorders [4, 5]. There is ample evidence that impaired hearing significantly limits communication abilities of an individual, directly or indirectly affecting their work productivity, emotional status, and overall quality-of-life [e.g., 5, 6].

Accurate and comprehensive assessment of the auditory function, appropriate prescription and fitting of an assistive device, and an effective aural rehabilitation program are all crucial for enhancing the communicative ability and restoring good quality of life for affected persons. This thesis concentrates on aspects related to hearing assessment, and details related to the assessment of auditory functioning are presented below.

1.2 Hearing Measurements

Assessment of the auditory functioning typically begins with the measurement of hearing sensitivity in different frequency regions. This test is most often performed by an Audiologist using an *audiometer*. The audiometer is an FDA-standardized medical equipment that usually consists of an embedded hardware unit connected to a pair of headphones, earphones, or speakers, and a feedback button [7]. Most audiometers are able to generate dual-channel audio signals for audiometric measurements on the left or right ear or both ears. Several features of the commonly available audiometers include: (a) ability to produce and control sounds at a variety of frequencies and intensities with different transducers, (b) ability to produce masking signals which will allow better testing of the individual ear, and (c) ability to carry out bone conduction measurements for quantifying conductive hearing loss [7]. The standard test types administered using the audiometer include puretone tests and speech tests, and these are briefly discussed below.

1.2.1 Puretone Audiometry and Speech Audiometry

Puretone Audiometry is used to identify hearing threshold levels of an individual. The stimulus signal varies from low pitches (250Hz) to high pitches (8 kHz). The results are displayed as a graph called *audiogram,* an example of which is shown in Figure 1-2.

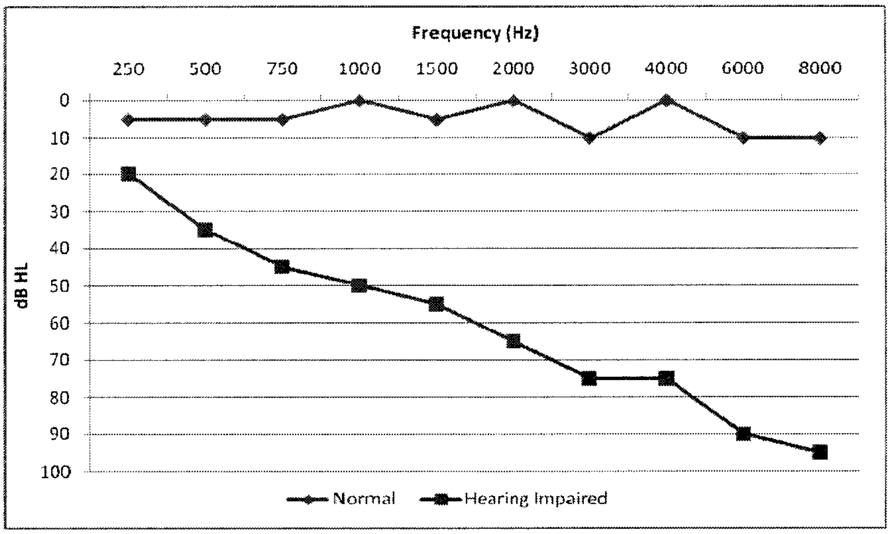

Figure 1-2: An Example Audiogram Showing Normal and Impaired Hearing Levels.

Figure 1-2 displays a typical audiogram obtained from a normal hearing listener and a hearing impaired listener with a high frequency sensorineural hearing loss. The ordinal axis in Figure 1-2 is expressed in dB Hearing Level (dB HL): a 0 dB HL value at all frequencies implies perfect normal hearing. Typically if the subject is within 20 dB HL he/she is judged to have "normal" hearing, and thresholds outside of this boundary are treated as hearing loss [7].

While the audiogram is primary evidence collected to diagnose hearing impairment, it is important to note that puretone audiometry only provides the patient's auditory sensitivity. In other words, this test describes what sounds an individual cannot hear, but fails to describe how well audible sounds are perceived. Perceived signal clarity and understanding of sounds is a function of many complex hearing abilities that are not reflected in the basic measures of sensitivity. In fact, adults and children with suspected central processing disorder often display normal hearing sensitivity [4, 5]. Thus, more comprehensive measurement of auditory functioning is required for proper evaluation of central processing auditory deficits.

Speech audiometry attempts to find out the patient's ability to hear and understand speech [7]. Spoken words and sentences are utilized instead of tones in speech audiometry. Examples of these tests include: (a) speech reception threshold (SRT) test that measures the softest sound level at which short words can be heard and understood at least half the time, (b) word recognition tests that determine the ability to understand single syllable words, and (c) speech in noise (SIN) or hearing in noise (HINT) tests that evaluate the subjects' ability to understand speech sentences in the presence of background noise. While these tests are better in probing the auditory functioning, they assume familiarity with words and sentences that are used in tests, and may not be applicable to all ages [7].

1.2.2 Psychoacoustic Measurements

Psychoacoustic measurements go beyond the audiogram and attempt to assess complex auditory functions such as auditory discrimination, speech perception in challenging acoustical environments, and sound localization and lateralization. Typical psychoacoustic measurements include:

- Measurements of frequency discrimination – these tests aim to quantify the ability of the listener to discriminate between two sounds of different frequency. The smallest detectable change in frequency is called the frequency difference limen [3]. During measurement, on each trial, the tones are presented in a random order and the listener is required to indicate whether the first or second is higher in frequency. The frequency difference between the two tones is adjusted until the listener achieves a criterion percentage correct, for example 75%. This measurement will be called the DLF (Difference Limen for Frequency) [3]. There is evidence that the frequency discrimination results can assist in the diagnosis of central auditory processing disorders. It has been shown that children with central auditory disorders show elevated frequency discrimination thresholds when compared to similarly aged normal controls [8, 9].
- Measurements of temporal resolution – these tests quantify the ability of the listener to detect changes in the temporal properties of the auditory stimulus. Two examples of temporal resolution tests include gap detection and temporal modulation transfer function (TMTF). Gap detection is used to measure the ability to follow rapid changes over time [3]. There are two types of signals to mark the gaps: bandpass-filtered noises and sinusoids. The measurement process is similar to measurement of frequency discrimination. The threshold for gap detection is the duration of the gap which is adjusted to find the point where it is just detectable. The function which relates threshold to modulation rate is called the temporal modulation transfer function (TMTF) [3, 10]. In the

simple case, the amplitude of a white noise signal is modulated sinusoidally, and the amount of modulation required to detect the modulation is determined as a function of modulation rate [3, 10]. As with the frequency discrimination tests, temporal resolution tests such as the gap detection test and TMTF allow for the diagnosis of auditory processing disorder and auditory neuropathy [11, 12, 13].

- Measurements of binaural processing - these tests quantify the ability of the listener in combining and processing the information acquired from the auditory stimuli presented to both left and right ears. Examples of these measurements include dichotic listening tests where different sentences are delivered to the left and right ears and the subject asked to identify both of the sentences, and binaural masking level difference (BMLD) tests where the improvement in signal detection in the presence of background noise due to binaural fusion is quantified.

In summary, there is enough evidence that more comprehensive diagnostic tests ought to be done to fully characterize the auditory function and dysfunction, and psychoacoustic measurements provide the bases for this comprehensive characterization.

1.3 Current State-of-the-Art

The current state-of-the-art for conducting psychoacoustic measurements is relatively backward compared to the technological advances in hearing aids, assistive listening devices, and other audiology diagnostic equipment such as auditory brainstem response (ABR) and otoacoustic emissions (OAE) equipment.

Currently the psychoacoustic tests are distributed on a CD by Auditec, a company based in USA [14]. For example, the central auditory processing test battery, which includes measures of frequency resolution, temporal resolution, and binaural processing, is sold on a single CD along with a set of instructions and scoring forms for $549 US. Similar bundled tests are available from Auditec for a variety of psychoacoustic measurements, where the clinician has to manually run the test, score the results and tally them.

The current generation audiometers do allow measurements of frequency and temporal resolution. However, it requires a substantial amount of effort from the clinician in order to run these tests manually and extract meaningful information from the results. In a busy clinic, this additional effort is often a deterrent to routine clinical use of psychoacoustic tests.

A number of research laboratories have developed customized hardware and software components for running a variety of psychoacoustic tests. For example, a number of psychoacousticians employ the modular hardware by the Tucker Davis Technologies (TDT), USA, together with customized software modules to drive the TDT equipment [15]. Figure 1-3 displays a version of the TDT-based psychoacoustic measurement system that is in use at the Children Hearing Research Laboratory at the National Centre for Audiology.

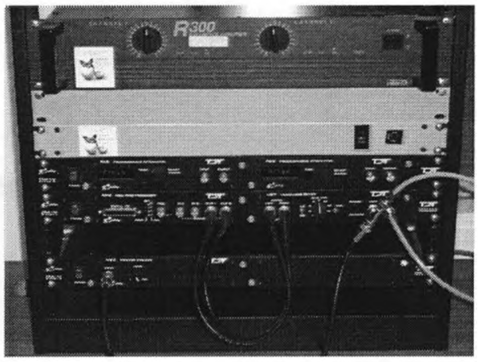

Figure 1-3: An Example of TDT Equipment for Psychoacoustic Measurements

In this figure, the software on the left runs the psychoacoustic test protocol, while the audio data conversion, level control, and transducer interface is provided by the TDT equipment on the right. This solution is viable only in research laboratories, and is difficult to migrate to a general Audiology clinic. Moreover, the TDT-based solution is not portable, and is not flexible to the addition of new tests. Note that portability is important as it allows psychoacoustic measurements in the field, e.g. testing children in schools, and testing older adults in nursing homes etc.

There have been advances in the development of portable and wireless audiometric solutions. Otovation, USA, manufactures the Otopod, a Bluetooth – based wireless audio interface to a variety of transducers. The company also developed the Symphony software that communicates with the Otopod and controls the signal delivery aspects. The key limitation of this system is its inability to stream arbitrary audio data over the wireless channel. The stimuli used for audiometric testing using this device are stored on a secure digital (SD) card and therefore form a restricted set. Moreover, the software comprises of basic pure tone and speech audiometry and does not include advanced psychoacoustic tests.

1.4 Problem Statement, Thesis Objectives, and Thesis Organization

There is mounting evidence that advanced psychoacoustic measurements of frequency resolution, temporal resolution, and binaural processing are essential for accurately determining the functioning of the auditory modality. Currently available clinical solutions for psychoacoustic measurements suffer from such key limitations as: (a) lack of automating the test administration, data collection, and data reporting, and (b) lack of flexibility and portability. Thus there is a need for developing clinically viable solutions for efficient administration of psychoacoustic tests.

The goals of the project were to design and implement a wired and wireless psychoacoustic 2-channel (stereo) testing systems. The rationale for the design of two different versions is as follows: the wired device is designed for in-clinic operation, where it will interface with the existing audiometer in the clinic. This is attractive as the existing audiometer and the associated infrastructure (sound booth, transducers, sound field setup) in the clinic can be used, together with the automation and flexibility developed with the wired device. The wireless version is designed for use in the field – a handheld computer (such as HP Pocket PC or the new mobile internet devices such as the Nokia N800) can be used to run the psychoacoustic measurement software, while the wireless hardware allows for level control, audio data delivery, and transducer interface.

The organization of thesis is as follows: Chapter 2 will detail the selection of the design plan. Chapter 3 will describe the hardware designs of the proposed systems in detail. Chapter 4 will present the process of firmware development. Chapter 5 discusses the RF measurement, as well as the objective and subjective evaluations of the proposed systems. Chapter 6 shows conclusions from this thesis work, summarizes the major contributions, and suggestions for future work.

Chapter 2

Design Plan Selection

Design plan selection was the first phase of our designs. Since there are many potential solutions in market for our project, considerable amount of time was spent on this part of the research.

2.1 Design Specifics

As mentioned in the previous chapter, there were two separate designs in this project. Figure 2-1 provides the conceptual overview of the wired and wireless versions of our psychoacoustic measurement system.

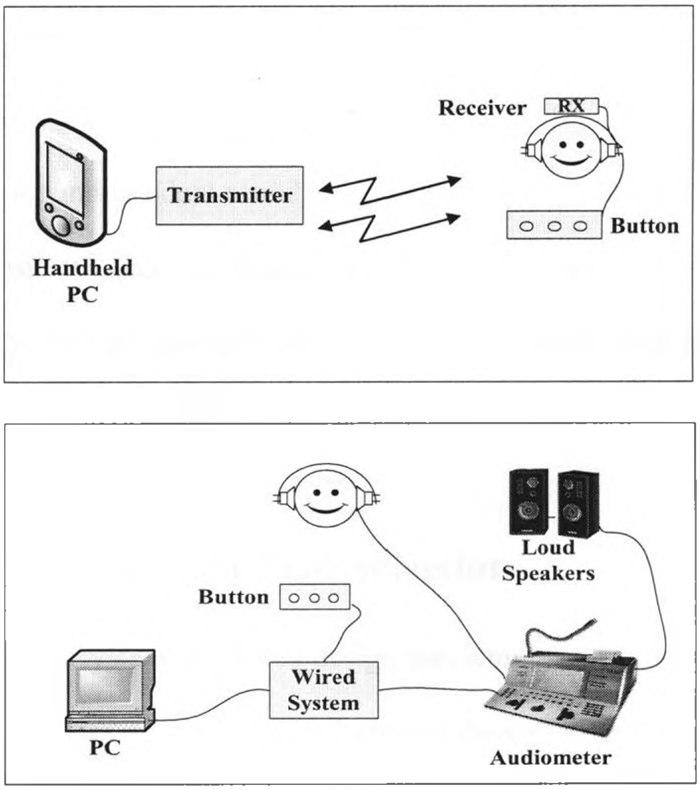

Figure 2-1: Conceptual Overview of Wireless and Wired Systems for Psychoacoustic Testing

As briefly discussed earlier, the wired hardware interfaces with an existing audiometer in a clinic. The application software residing on a host PC delivers digital audio and level control data to the wired device, which then performs the required digital-to-analog conversion and delivers it to the audiometer, which in turn presents the audio signal through headphones or loudspeakers. The wireless system, on the other hand, is designed for field use. Here the application software residing on a portable computer delivers digital audio and control data to the transmitter, which streams this information over to the receiver. The receiver decodes this information and delivers the precisely controlled audio signal to headphones. Within this conceptual framework, following design guidelines were developed to meet the goals of the psychoacoustic testing system:

- integrated button response function. The testee can respond to the sound coming from the host by pressing corresponding button and the host is able to detect these signals.
- high quality audio signal that spans the entire 20 Hz – 20 kHz bandwidth.
- precise and independent sound level controls on the left and right channels.
- robust performance in diverse wireless environments, where the wireless system is able to maintain satisfactory audio quality over time during normal operation, even if interference sources exist.

2.2 Wired System Design Plan Selection

Compared to wireless system, the wired design was simple and straightforward. The data transferred with host are audio signal and control data such as sound level and button response.

2.2.1 Audio Data Format Selection

Among computer peripherals, a soundcard is the conventional sound equipment. However, built-in soundcards in commonly available laptops and desktops are susceptible to noise and interference from other subsystems (video card for example). As an example, we observed 122mVpp noise from a 40Ω headphone connected with a laptop. Compared to an internal soundcard, the USB audio format is a better choice as it offers better noise immunity. The isochronous transfer type in USB protocol was specifically designed to support audio. USB transmits frame from the PC host at a 1 ms rate, and an isochronous IO device will receive data in every frame. In our design, CD-quality sound at 16 bits and a sample rate of 44.1 kHz need 176.4 bytes of data transferred in 1 ms frame. The IO device would receive this data, buffer it and play them back [16].

2.2.2 Sound Level Control Data and Button Response Data Formats Selection

In order to achieve accurate sound levels, we included an external attenuator to change the volume in the design. The HID class within USB classification consists primarily of devices that are used by humans to control the operation of computer systems. Many USB audio chips have GPIO Pins with Read/Write facility via the HID Interface, which facilitates the transfer of control data. Therefore, the USB HID interface was used to transmit both sound attenuation and button response data.

2.3 Wireless System Design Plan Selection

The wireless system utilizes the same host interface protocol for audio and controlling data in wired system. In addition, there were more other options we had to choose for the wireless system.

2.3.1 Wireless Band Selection

There are many alternatives from traditional 27MHz solution to the popular 2.4GHz solution to choose for the design. In our design, the following requirements were set to the application: Firstly, we had to consider the base bandwidth of the audio signal. The base bandwidth of the audio signal is 44100 sample/second *16 bits/sample * 2 channel=1.4112 Mbit/second. Secondly, compact size was needed. Therefore, the antenna size is a crucial factor. In addition, a free license band is preferred.

In comparison to lower frequency bands, the 2.4 GHz band is wide allowing for much higher data rates and a variety of RF solutions to operate within the same frequency band. Due to the higher frequency, the 2.4GHz antenna is around 30mm (1/4 λ), and the 2.4 GHz band is free licensed. Therefore, the 2.4 GHz wireless band is the best candidate for us.

2.3.2 Wireless Protocol Selection

Compared to wired communication, wireless equipments suffer from path loss, interference and multipath propagation. Furthermore, the 2.4 GHz license-free band is attractive for use by various commercial applications and communication protocols. For example, the Wireless Local Area Network (WLAN), Bluetooth and cordless telephones, all inhabit the 2.4 GHz spectrum. Consequently, the devices working in this band are subject to interference from each other. Therefore, we had to choose an appropriate protocol from the various available wireless protocols for our system.

2.3.2.1 Option A: Bluetooth

The Bluetooth RF operates in the unlicensed ISM band at 2.4GHz. The system employs a frequency hop transceiver to combat interference and fading, and provides many FHSS [17]. High quality audio (stereo or mono) can be streamed from one device to another over a Bluetooth connection. The Bluetooth Special Interest Group (SIG) published the specification as "Bluetooth 2.0 + EDR" on November 10, 2004 which implies that Enhanced Data Rate [EDR] is an optional feature. It is capable of providing 3Mbps. Bluetooth is a standard and communications protocol primarily designed for low power consumption, with a short range (power-class-dependent: 1 meter, 10 meters, 100 meters) based on low-cost transceiver microchips in each device [17].

However, there are some drawbacks with the Bluetooth option:

1. Bluetooth chips are quite expensive. For example, the F2M03ALA is a low power embedded Bluetooth™ v2.1+EDR audio module with an on board antenna, integrated audio codec and amplifier. The module is fully Bluetooth™ qualified as an end product requiring no additional qualification. With a transmit power of up to +4 dBm and receiver sensitivity of down to –86 dBm combined with audio codec and low power consumption [18]. But the price is more than 70 CAD each.

2. Bluetooth chips have large size. For example, F2M03ALA is 24x13x2.1mm and 39 pin package [18]. However, in this design, due to the size limitation, small chip package is an important requirement.
3. The Bluetooth chips available in the market when we started our project (October 2007) did not support transmission rate more than 1.4Mbps.
4. Many existing Bluetooth solutions suffer from poor audio quality due to the use of lossy audio compression. Our design goal was to provide CD-quality sound over the wireless channel.

2.3.2.2 Option B: IEEEE 802.11

IEEE 802.11 is a set of standards to carry out wireless local area network (WLAN) computer communication in the 2.4, 3.6 and 5 GHz frequency bands. The 802.11b protocol is used in most laptops and the maximum raw data rate is 11 Mbit/s.

It must be noted that IEEE802.11 is a protocol for wireless local area network. It works in two modes: infrastructure and ad-hoc mode. Access Point (AP) is employed in infrastructure mode or some devices have to act as AP in ad-hoc mode. Both of them would make our project more complicated. Another problem is that IEEE802.11 belongs to computer network protocols. If the existing network solutions were adopted, we had to suffer from much more overhead and as a result, complex circuit and high power consumption.

2.3.2.3 Option C: Kleer Wireless Audio Module KLR3012

Kleer is a relatively new fabless semiconductor company that manufactures wireless audio ICs. For example, the KLR3012 is a complete solution for high quality digital stereo audio over a robust RF link [19]. Its 2.37 Mbps peak rate is able to carry CD-quality stereo audio. Fully integrated RF filtering makes the peripheral circuit simple and provides 1.5dBm output power. The receive sensitivity is -87dBm. Since integrated 8-bit microcontroller, it supports hardware control, radio control and application functions. During the course of this project, the Kleer evaluation kit was ordered for our project. After evaluation, the RF and audio signal quality met our requirements. However, the attenuation control proved to be quite complicated and needs to reset the chip with 2 seconds delay which was not acceptable in our design. In addition, we were not able to control the chip because detailed register description was not provided.

2.3.2.4 Option D: Nordic nRF24Z1 2.4GHz Wireless Streamer

nRF24Z1 is a 4 Mbit/s single chip RF transceiver that operates in the world wide 2.4 GHz license free ISM band [20], with several advantages. For instance, the size is small with only 6x6mmm QFN package. The data speed in RF link is up to 4 Mbps. The chip provides a true single chip system for CD quality audio streaming of up to 16 bit 48 kSPS audio, and I2S and S/PDIF interfaces are supported for audio I/O. The digital audio data are different from analog signal which attenuates with distance. Hence, the audio signal converted by DAC is constant even the transceiver is moving. For digital interface, SPI or

I2C control serial interfaces are included. The power consumption is 23mA in receiving mode and 17mA in transmitting at 0dBm output power. From the nRF24Z1 Headphone reference design [20], the working distance is 10 meter line-of-sight range without RF power amplifier and this distance was adequate for our system.

After extensive research of these alternative technologies, we chose nRF24Z1 as the best solution of wireless transceiver chip.

Chapter 3

Hardware Design

This chapter discusses the hardware design in our projects. Because both wired system and wireless system consist of USB audio chip, microcontroller and attenuator, hence they will be presented first. The wireless system design is then discussed in detail. Both the wired and wireless designs were validated by estimating the current consumption and audio output level using PSpice before the real devices were built. PCB layout was designed for the systems and will be presented in this chapter as well.

3.1 Overview of the Hardware Systems

Because we designed two systems and some parts were same or similar, it is better to introduce wired system firstly due to its simple structure.

3.1.1 Wired Hardware System

The block diagram of the wired psychoacoustic test system is shown in Figure 3-1. It primarily consists of application software along with USB host driver, CM108 USB audio interface chip, LM1973 attenuator, and Mega8 microcontroller (MCU). The application software communicates with wired psychoacoustic test system, and displays test results. It transmits stereo audio data and control commands through a USB port to the wired system, based on the experiment chosen and the subject response. The

Graphical User Interface (GUI) on the host displays results and allows the user to easily select and modify parameters for different psychoacoustic tests.

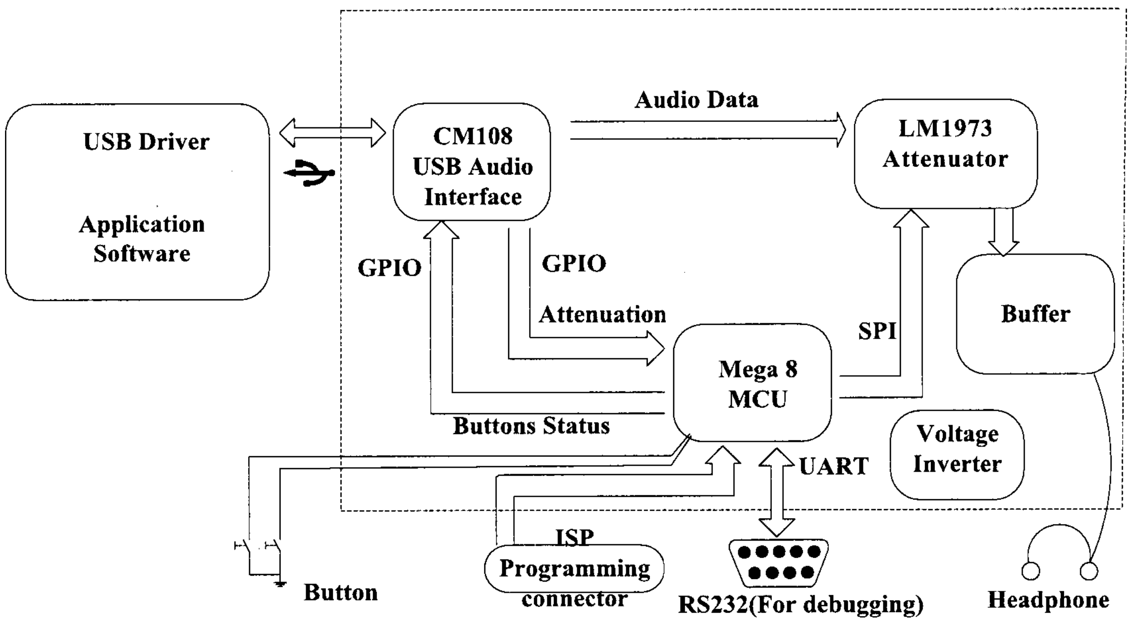

Figure 3-1 Wired Psychoacoustic Testing System

The USB interface chip, CM108, receives USB data from the USB port. It retrieves analog audio data and transfers them to the attenuator, LM1973, which controls the sound level. Although there are some microcontrollers integrated with USB interface, we chose CM108 + Mega8 in the design to guarantee high performance with a dedicated MCU. The MCU, Mega8, is the central controller. It coordinates the USB chip and the attenuation chip. In order to transmit the sound attenuation level signal and receive the status of the buttons, four GPIO (general purpose IO) pins in the CM108 act as two group signals: one group has 2 GPIO pins and transmits sound attenuation data from CM108 to Mega8. The MCU translates these two signals to SPI which connects to LM1973; the other group has another 2 pins and transmits buttons status data from the Mega8 which detects button status periodically. The system is powered by USB port. Voltage inverter MAX660 provides the needed -5V for attenuator and buffer, the functioning of which is detailed later in this chapter.

3.1.2 Wireless Hardware System

Figure 3-2 and Figure 3-3 show the block diagram of the wireless hardware for the psychoacoustic test system.

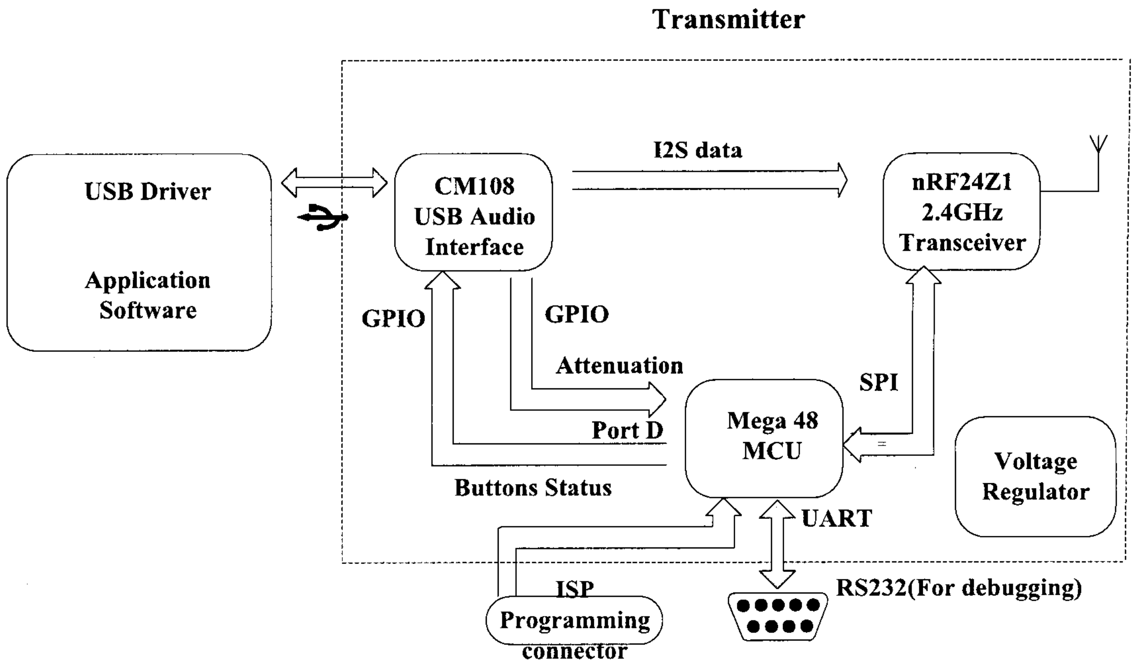

Figure 3-2 Transmitter Block Diagram

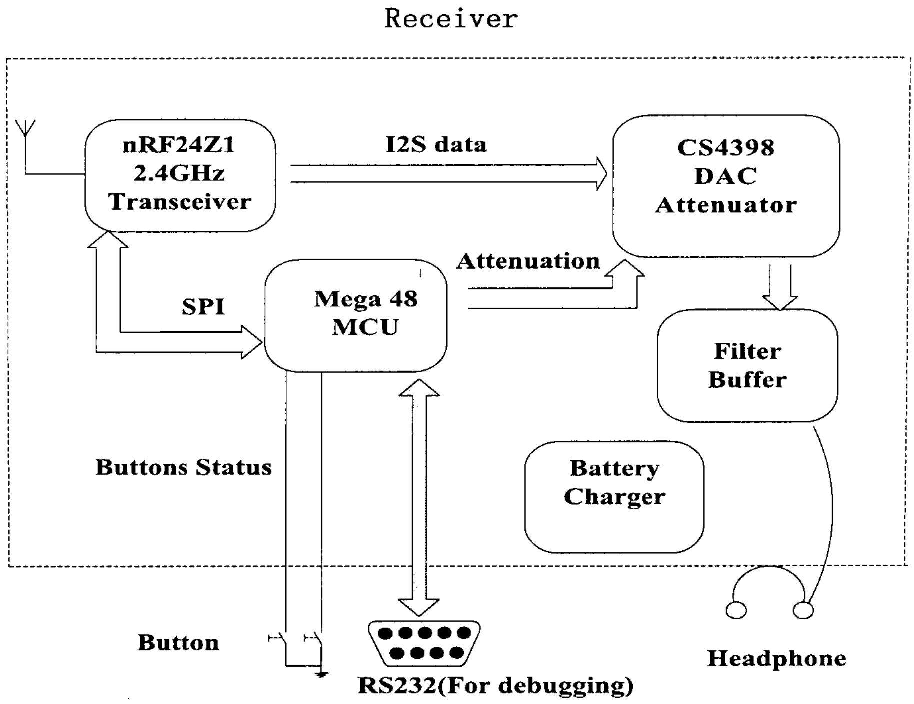

Figure 3-3 Receiver Block Diagram

We adopted USB + Microcontroller (ATMEL AVR Mega48)+2.4GHZ wireless IC(nRF24Z1) mode for wireless design. This system includes two subsystems: a transmitter and a receiver. The transmitter transmits stereo audio signal and sound attenuation signal to the receiver, and receives the status of the buttons from the receiver. The receiver receives the audio signal in the I2S format as well as the attenuation data, in addition to transmitting the status of response buttons.

The CM108 chip in the transmitter receives the USB data from a USB port. It extracts the digital audio data and transfers them to the wireless transceiver, nRF24Z1, in I2S format. The Mega48 controller was used instead of Mega8 because of the availability of more interrupt pins and low power dissipation. 2 GPIO pins in the CM108 send sound attenuation data from CM108 to Mega48; the other 2 GPIO pins transmit buttons status data from Mega48 to CM108. The MCU translates these two signals via SPI which is connected to the nRF24Z1 chip. Therefore, the RF signal is combined with the audio and the control data. Since all chips in the transmitter are working under 3.3V, one 3.3V power regulator was used to provide the power in transmitter.

On the receiver side, the wireless chip, nRF24Z1, receives the RF signal, decodes to I2S audio and feeds it to the Digital to Analog Converter (DAC). The DAC converts the digital data to analog audio which flows to the attenuator to get appropriate volume. In this design, the DAC and the attenuator are integrated in one IC, CS4398. The MCU also controls the data communication in the receiver. It responds to an interrupt triggered by the nRF24Z1 and decodes the sound attenuation data in SPI bus from the nRF24Z1, then puts it to the attenuator through I2C bus .The response signal from buttons are fed to the MCU as well. The MCU converts them to SPI signal, sends them to the nRF24Z1. In addition, an audio filter and buffer are employed to get high quality audio output.

Additionally, two power regulators are included in the receiver circuit, which provide ±5V for the attenuator and the buffer, and +3.3V for the MCU and the nRF24Z1 chip respectively. As the wireless system was designed for field operation, a Lithium battery and charging circuit are deployed in the design.

3.2 Debugging Consideration

Due to the complexity of communication data and 2.4 GHz wireless transmission in the design, debugging became an important issue and a very time-consuming process. To be more efficient, we had to use following methods and hardware to debug, although they were removed in final version.

LEDs were used to be connected to the GPIOs of USB audio chip CM108 for monitoring the attenuation and button data. Since the GPIOs can work at very slow speed in debugging mode, if the ports were asserted to high, the corresponding LEDs were on. Because the application software in host was developed at the same time, we can identify the bugs whether from the host application software or the transceiver side by visually watching the LEDs.

After embedding an MAX3232 RS-232 line driver/receiver IC in design and taking an RS-232 cable connecting the transmitter/receiver to a PC with setting proper baud rate, we were able to monitor the data coming from the wireless system. As discussed in Chapter 4, there were many branches in the firmware, and it was imperative to figure out whether the specific codes were executed or not. By putting short codes in firmware which can transmit specific words such as "branch A executed" to the PC through RS-232, this problem was solved easily. As controlling the nRF24Z1 is based on reading and writing its internal registers, it was very effective to access these registers in nRF24Z1 from PC side using serial debugging software.

3.3 USB Protocol Introduction

USB is a very popular protocol connecting peripherals with PC. It is capable of transmitting many types of data such as video, audio in high speed. A USB interface includes power supply pins, providing +5V with maximum 500mA to devices. Hence, it is attractive that the wired system and the transmitter of the wireless system can be powered by USB. It also supports hot plug, which means the audiologist can connect and disconnect the systems to host whenever he/she wants. These advantages make the hardware set-up easy and quick.

USB operates using client-server architecture where the bus is controlled by a host controller. When devices are attached to the bus, the host initiates communication with the device, assigns an address to the device and then controls all transfers to and from the device. A USB IN transaction is data transferred into the host and an OUT transaction is data transferred out of the host. Details of the USB protocol can be found in [16].

3.4 USB Audio I/O Controller: CM108

As mentioned in chapter one, there are two headphone channels (stereo) in our systems for psychoacoustic testing. We chose C-media's CM108 as the USB audio controller in our system.

3.4.1 Features of CM108

CM108 is a highly integrated single chip USB audio solution. All essential analog modules are embedded in CM108; including dual DAC and 32ohm earphone driver which means the output impedance is very low. For value added application, external codec can be connected to CM108 via I2S for further processing. In wireless design, we employed I2S as digital audio data format. It has 4 GPIO Pins with Read/Write facility via HID Interface which we used to transmit attenuation data and button status. The standard 44.1 kHz sampling rate (CD quality) for playback was adopted in our design. The chip is compatible with Win98 SE / Win ME / Win 2000 / Win XP and Mac OS9 /

OS X without an additional driver [22]. The typical power consumption is 27 mA as we measured.

3.4.2 Schematics of CM108 in Designs

In the wired system design, we used the CM108 analog output directly. In contrast, the I2S output was used in the wireless system. An LED was connected to Pin12 to indicate the USB port status. To decrease the size, USB Mini-B interface was chosen to connect with the host. The schematics of CM108 in wired system and wireless transmitter are shown in Figure 3-4 and 3-5.

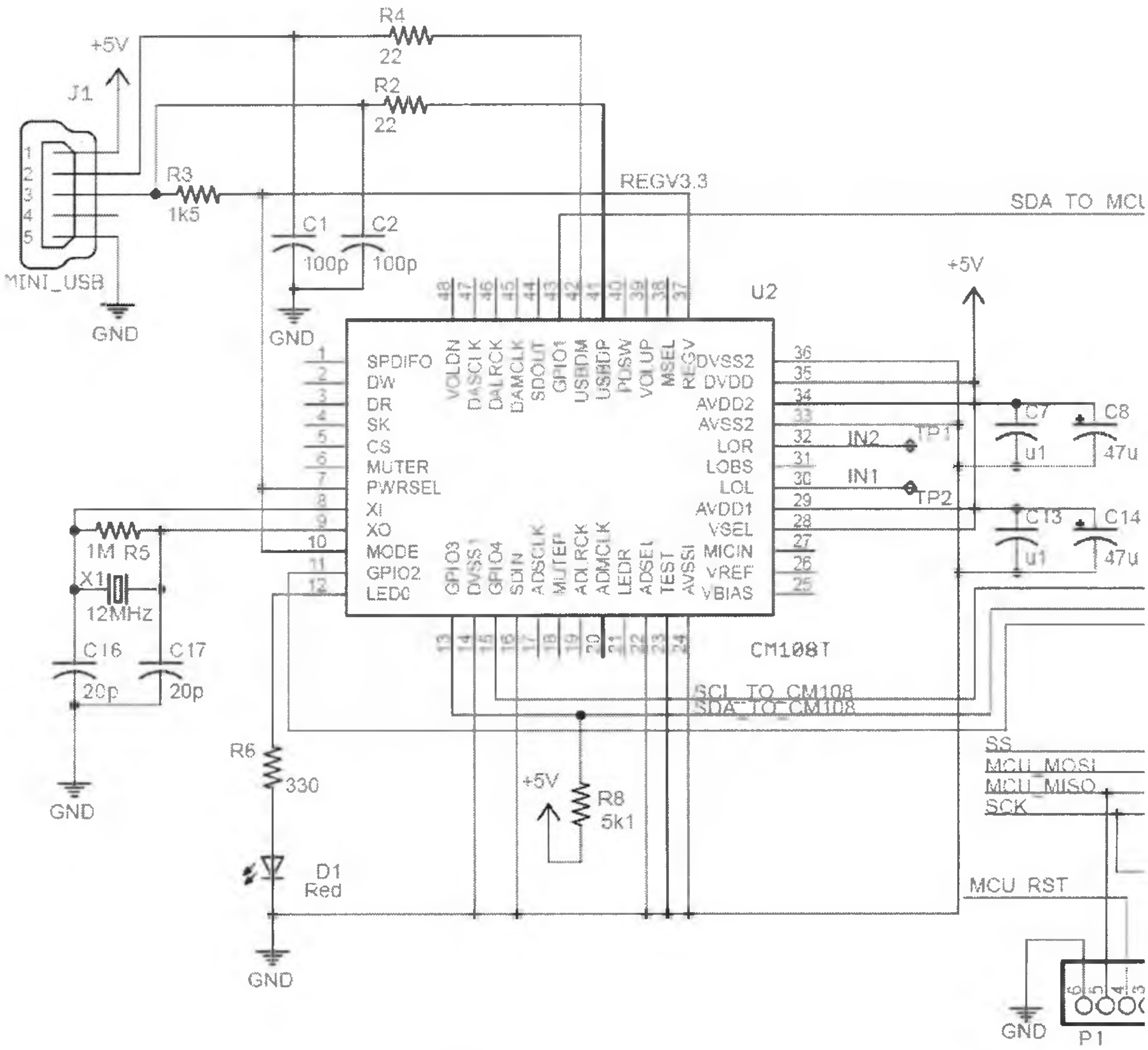

Figure 3-4 CM108 Schematic in Wired System

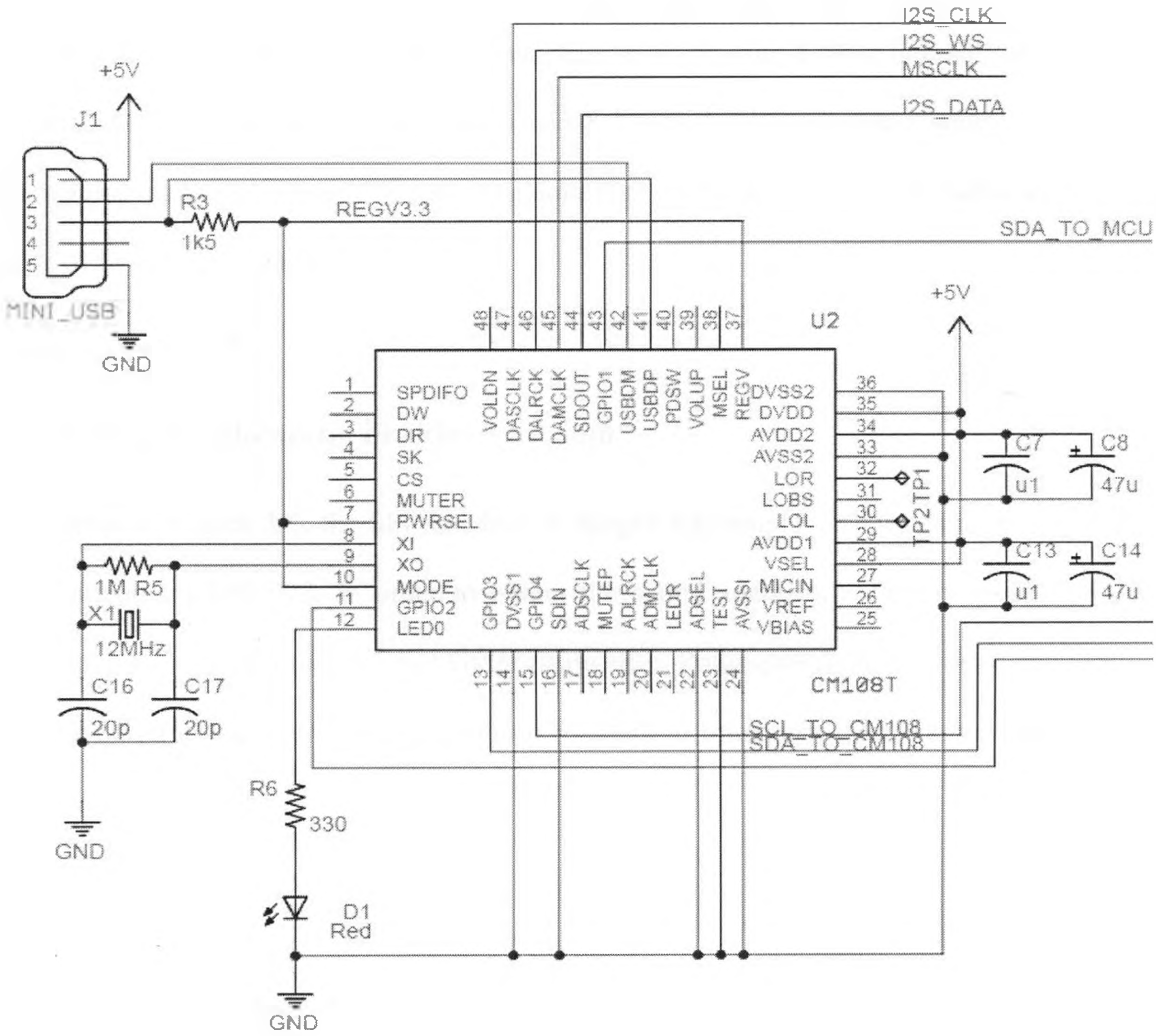

Figure 3-5 CM108 schematic in Wireless Transmitter

3.5 Microcontrollers in Both Designs: Atmel AVR Mega8 and Mega48

ATmega48 and ATmega8 are low-power CMOS 8-bit microcontrollers based on the AVR enhanced RISC architecture. By executing powerful instructions in a single clock cycle, the ATmega8 and Mega48 achieve throughputs approaching 1 MIPS per MHz which allows the system designer to optimize power consumption versus processing speed [23, 24]. In both systems, microcontrollers were set with 8 MHz internal oscillator so that the achieved throughputs approached 8 MIPS; UART interfaces were used for debugging purpose; ISP (In-System Programming) connector was also included for the ease of firmware upgrading.

3.5.1 Mega8 Schematic in Wired System

As shown in Figure 3-6, the SPI interface in Mega8 was employed for communications with attenuator LM1973. In order to obtain the sound attenuation data from CM108, INT0 and INT1 were used to detect GPIO rising edge. Polling mechanism was adopted to scan the button status and internal pull-up resisters in microcontroller were enabled to connect the buttons.

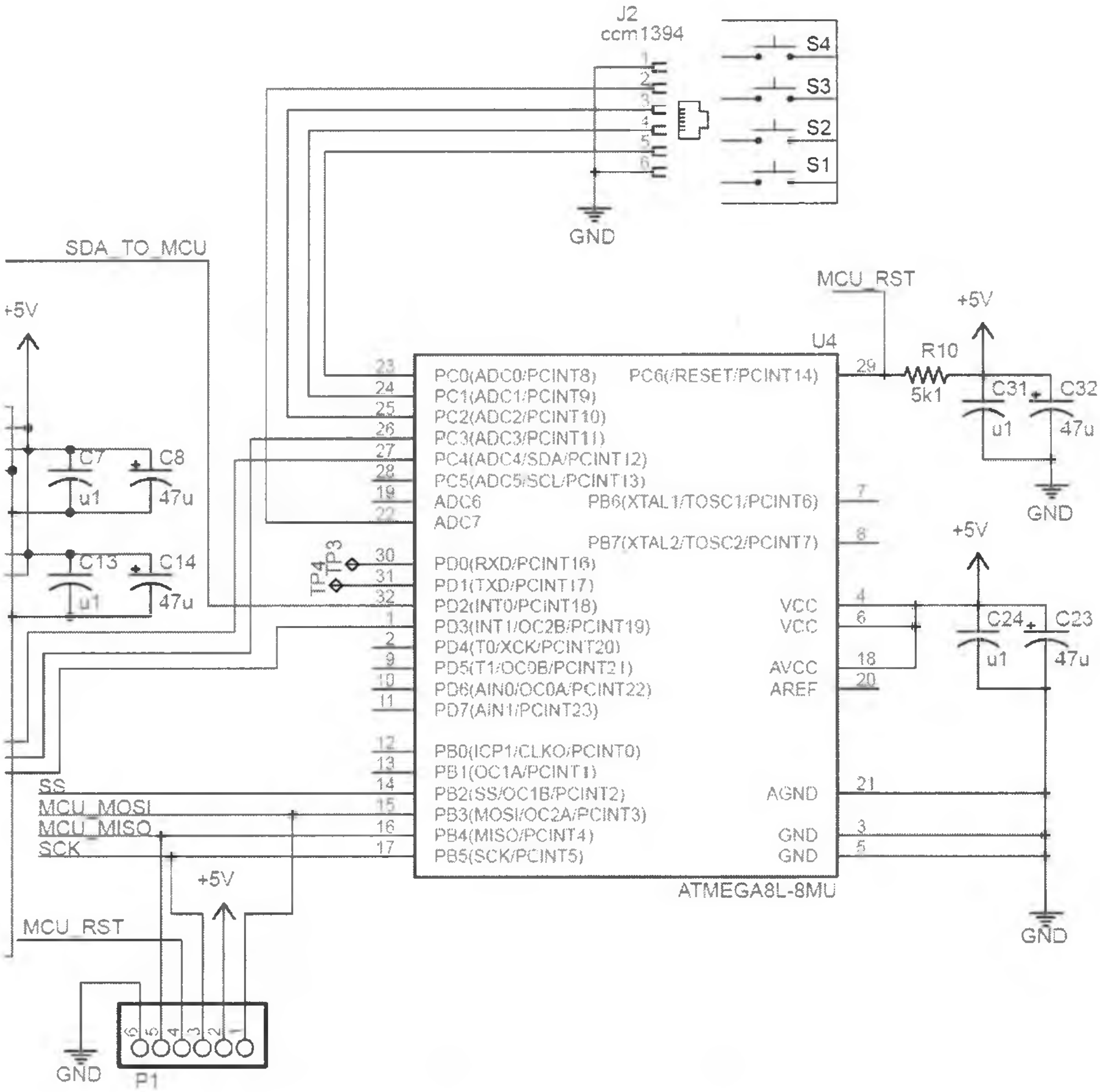

Figure 3-6 Mega8 Schematic in Wired System

3.5.2 Mega48 Schematic in Transmitter

On the transmitter side, Mega 48 communicates with the wireless chip through SPI protocol. To obtain the sound level data from CM108, the attenuation data were detected by INT0 and INT1. PCINT0 was used to detect the interrupt from nRF24Z1 when it received the button response data. The schematic is shown in Figure 3-7.

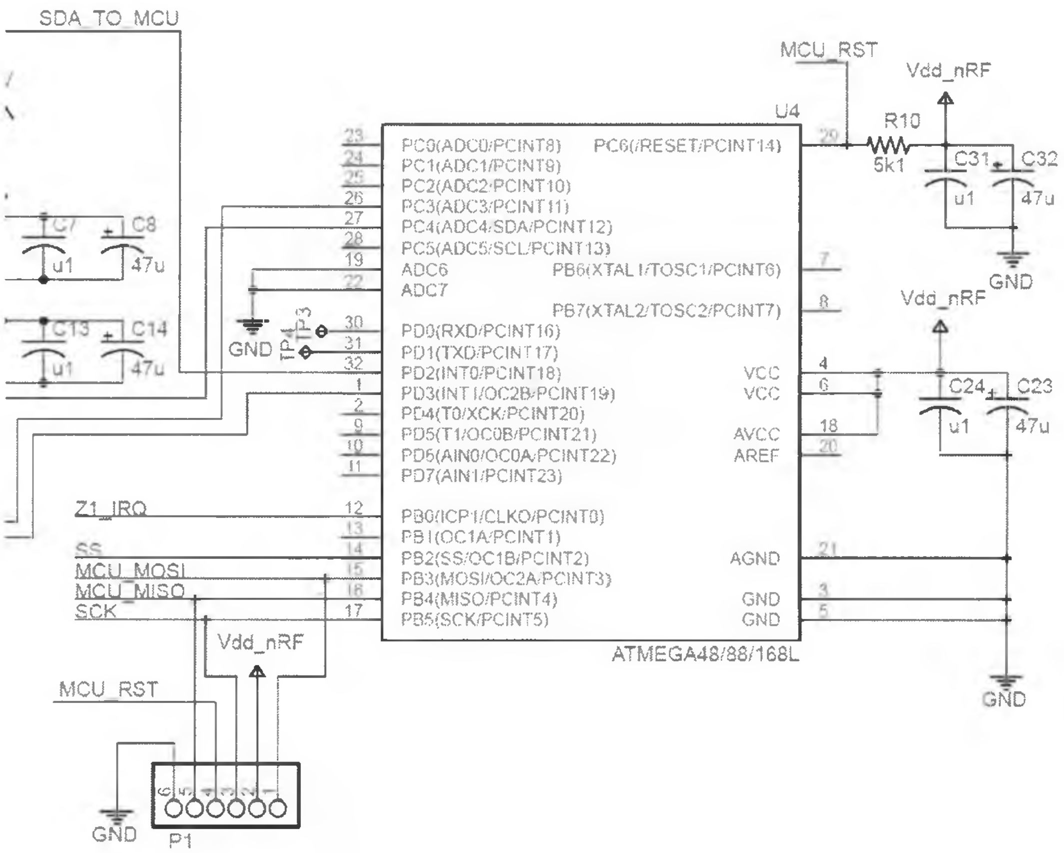

Figure 3-7 Mega48 Schematic in Transmitter

3.5.3 Mega48 Schematic in Receiver

Figure 3-8 shows the Mega48 schematic in receiver. I2C and SPI interfaces in Mega 48 were used for communications with the wireless chip and the DAC chip. INT0 was used to detect IRQ (Interrupt Request) coming from nRF24Z1 which attained the sound attenuation data from transmitter side.

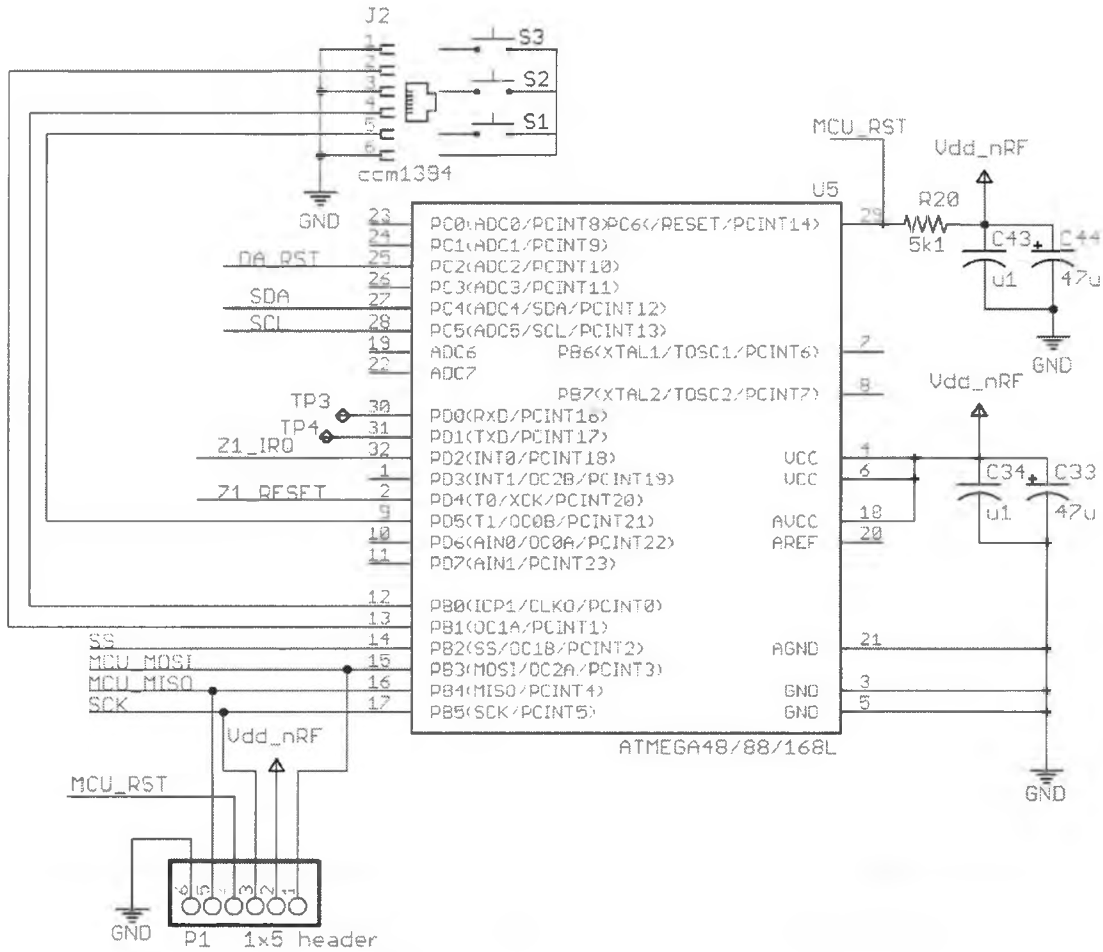

Figure 3-8 Mega48 Schematic in Receiver

3.6 LM1973, Unity-gain Buffer and Simulation in Wired System

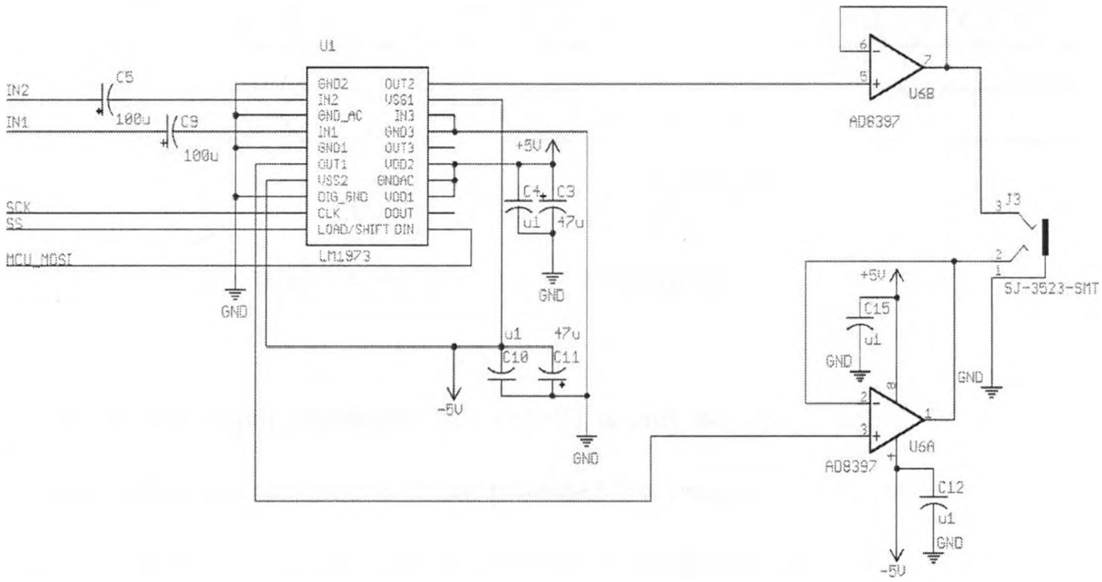

Figure 3-9 LM1973 and Unity-gain Buffer Schematic

Figure 3-9 shows the schematic of LM1973 and unity-gain buffer. We chose LM1973 as the attenuator in wired system because it is a digitally controlled 76dB audio attenuator. Each channel has attenuation step of 0.5dB from 0-15.5dB, 1.0dB steps from 16db 47dB and 2.0dB steps from 48dB-76dB. The working current is 3mA typically [25]. The input impedance is constant at a nominal 40kΩ. Therefore, LM1973 can connect to CM108 directly since CM108 is able to drive 32Ω headphone and its impedance is very low. It uses a 3-wire serial communication which can be implemented by SPI. Figure 3-10 illustrates the control timing.

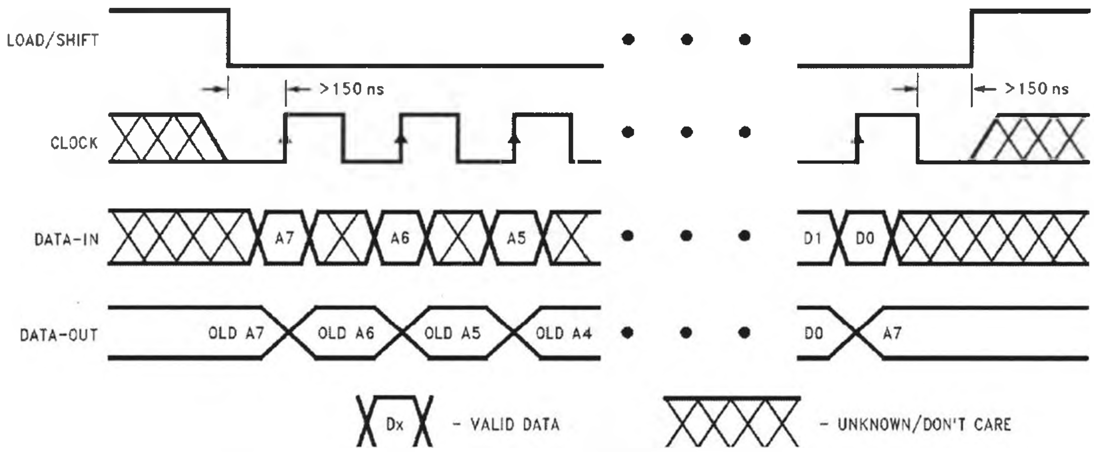

Figure 3-10 LM1973 Control Timing [25]

Since the output impedance of LM1973 is only between 25kΩ and 35kΩ [25], a unity-gain buffer was attached to it and provided low output impedance to headphone as well as very high input impedance to LM1973. Considering the headphone is 40Ω, we used rail-to-rail, high output current amplifier AD8397. Its static current is 8.5mA and its maximum output current is 250mA when Rload=12Ω [26]. The CM108 chip provides a maximum 1.25 Vrms audio signal [22]. We converted the AD8397 SPICE model to PSpice model and drew the schematic shown in Figure 3-11.

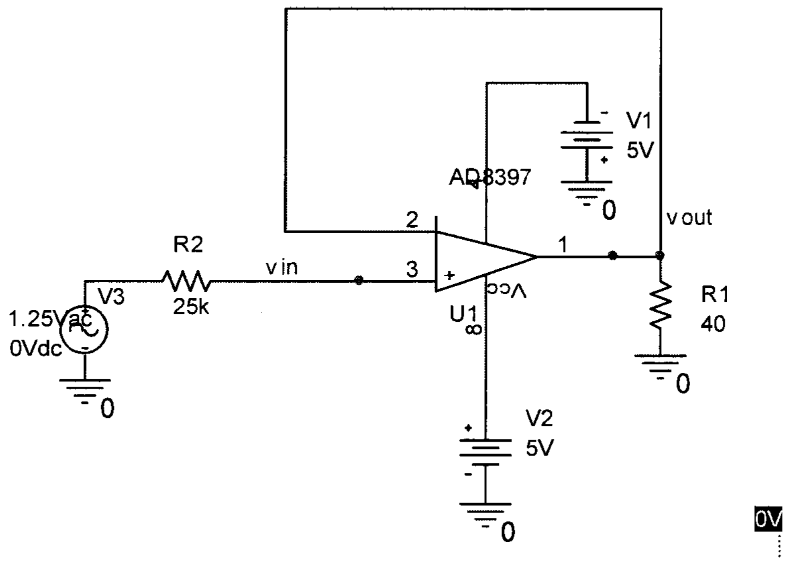

Figure 3-11 Schematic of AD8397 for Simulation (Assuming Vrms is 1.25v)

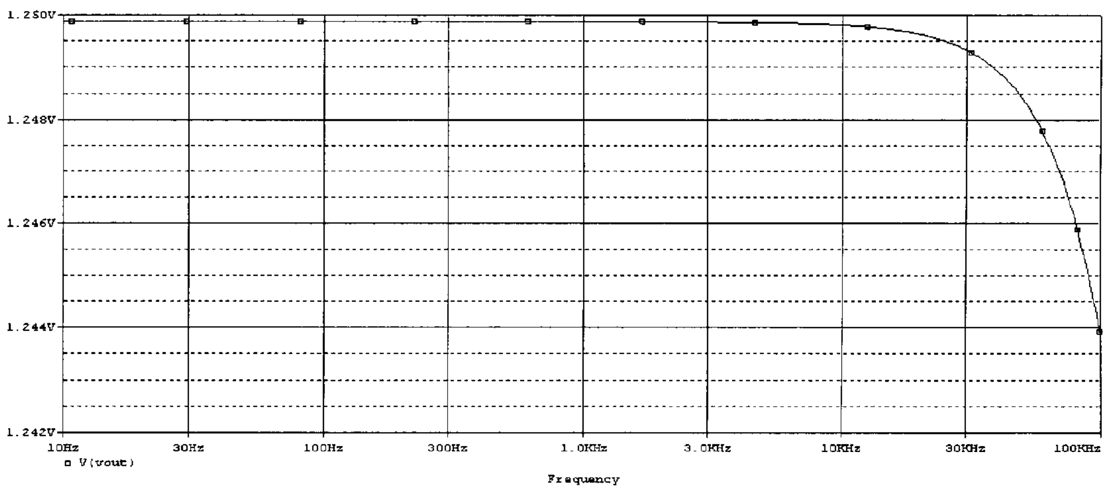

Figure 3-12 Simulation Result of Frequency Response

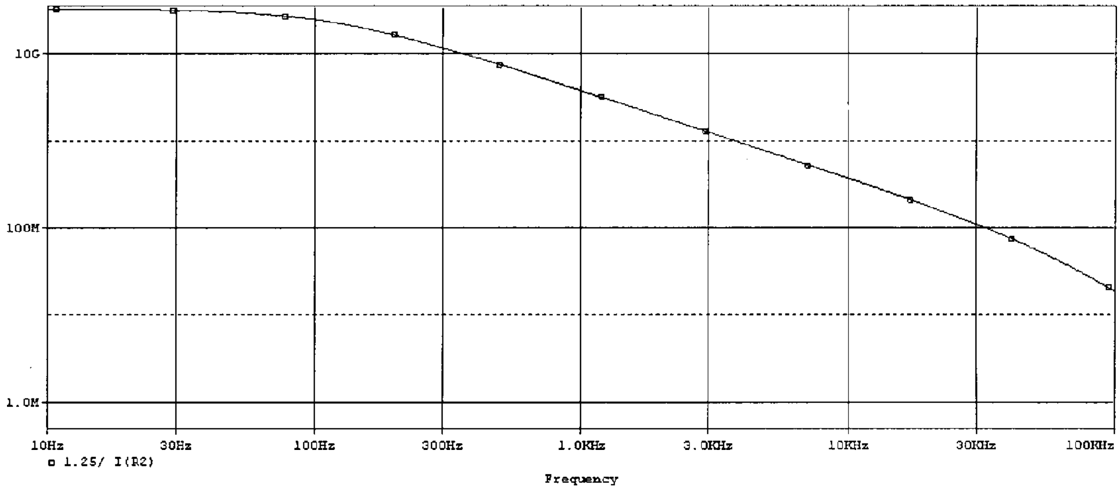

Figure 3-13 Simulation Result of Input Impedance

From the simulation results in Figure 3-12 and Figure 3-13, the output from AD8397 is almost 1.25Vrms and as same as the input value even the frequency is 100 kHz. The input impedance of the buffer is larger than 1MΩ. To demonstrate that this level is sufficient, consider the Sennheiser HDA 200 (a common wide bandwidth headphone used in audiometric applications [27]) which generates 108.5 dB of SPL (Sound Pressure Level) at 1 kHz with 0.5 Vrms drive [27]. Consequently, the audio output level meets the hearing test requirement.

3.7 Power Converter MAX660 and Total Current Estimation

Since the attenuator and unity-gain buffer need -5V power, the maximum power on the load=U*U/R=1.25*1.25/40=39mW in theory, and the average power from the -5V power supply =39/2=19.5mW. The average current of -5V power supply=P/U=19.5/5≈4 mA. We chose MAX660 as the power converter since the output current of MAX660 is at least 100mA@-5v and the output impedance is typically 6.5Ω [28].

Because the Mega8 active current is 6 mA[13], supply current to AD8397 is 8.5mA for 5v and -5V[16], ideally, the total current drawn by the wired system

$I_{total}=I_{cm108}+I_{ad8397}+I_{mega8}+I_{lm1973}=27+(4+4+8.5+8.5)+6+(3+3)=64$ mA

The actual current should be larger since the efficiencies of AD8397 and MAX660 are less than 100% and the values we used are typical values. But since the USB port is able to provide 500mA@5v, even taking into account of some practicalities of power consumption, the complete wired device can be powered through the USB.

3.8 2.4GHz Wireless Audio Streamer nRF24Z1 in Transmitter and Receiver of Wireless System

In the wireless system design, CM108 feeds data to nRF24Z1 using standard audio format (I2S). The nRF24Z1 pair transfers audio data from the source and present it to a stereo DAC on the receiver. Application-wise, the nRF24Z1 link will appear as an open channel (like a cable). Initial configuration of nRF24Z1 was done by the Mega48 through an SPI control interface. On the destination side, a DAC & Attenuator is controlled from the audio source side through the control channel offered by the nRF24Z1 chip.

3.8.1 Communication and Data Transfer Principle

To differentiate between audio data and other control and status data, the data traffic between the ATX and ARX has been organized in two data channels.

3.8.1.1 Data Channel Definition

The *audio channel* is defined as the communication channel sourcing audio data from the ATX to the ARX. The audio data is divided into two categories; real time data from the audio source and retransmitted audio information. When audio information is lost, the ARX requests retransmission of the lost packets. Real time audio bit rate is constant, whereas the amount of retransmitted audio varies over time [29].

The nRF24Z1 *control channel* is a two-way, low data rate channel superimposed on the audio stream. The audio transmitter is the designated master, meaning that when an RF link is active, the 2-wire, SPI, GPIO and internal registers in the audio receiver can be seen and controlled as a virtual extension of the audio transmitter's own I/O and registers. The implications of this is that external devices like audio DAC or volume control components connected to the audio receiver effectively can be controlled by input to the ATX. User actions (i.e. push of a button) on the audio receiver side are similarly fed back to and can be processed on the audio transmitter side [29]. Figure 3-14 shows nRF24Z1 communication channel principle.

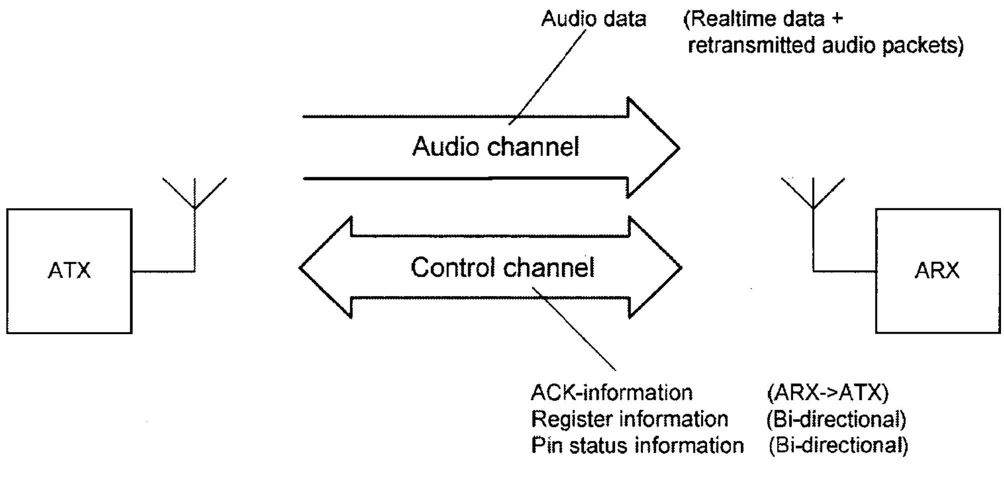

Figure 3-14 nRF24Z1 Communication Channel Principle [29]

3.8.1.2 Data Flow and Organization

Figure 3-15 illustrates the communication principle of an nF24Z1 wireless link. Data is transmitted from the ATX to the ARX on a cyclic basis. ATX data are organized in frames transmitted with frequency 1/tp. A data frame contains the real time audio data and retransmitted audio data requested by the ARX. Poor operating conditions (i.e. excessive range and/or high amount of interference) will result in a higher amount of retransmitted audio data a frame [29]. Figure 3-15 also illustrates how period length, frame size and retransmission capacity varies with sample rate and time [29].

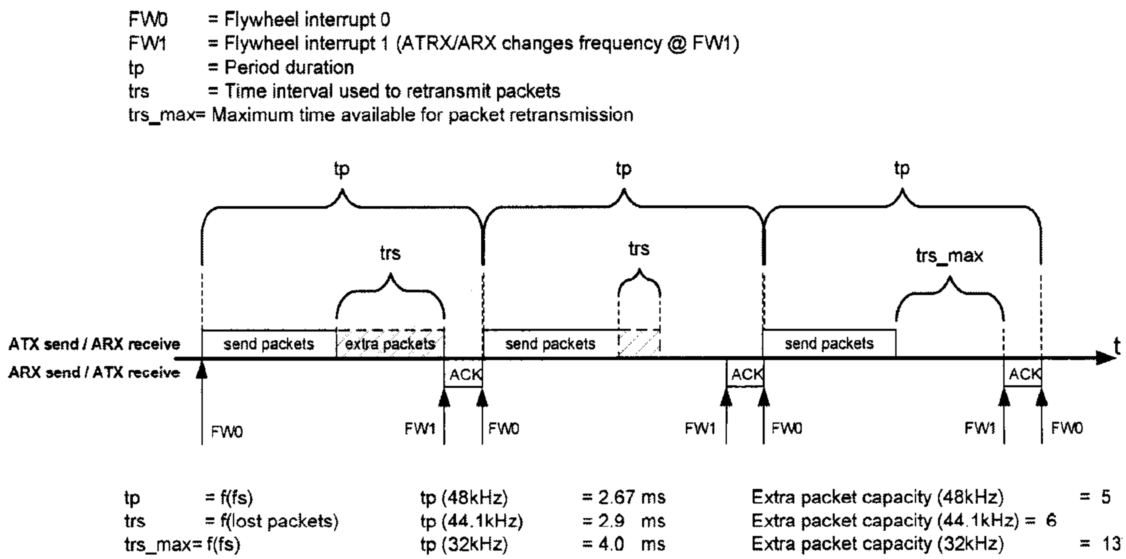

Figure 3-15 nRF24Z1 Data Streaming Principle [29]

As shown in Figure 3-16, audio data is organized in *stereo samples* (SS). The stereo samples are in turn organized in data *packets* consisting of 16 stereo samples. A data packet also contain preamble, recipient address, packet id, compression information, CRC-string and a limited amount of control and register data. A data *frame* consists of a segment of real time data. In addition, the frame contains audio packets requested by the ARX for retransmission. The maximum number of packets for retransmission depends on the sample rate of choice. When the ARX has received the data frame, an *acknowledge packet* is generated and sent to the ATX. This packet consists of acknowledge information (requesting retransmission of corrupt/lost packets) and control and status information [29].

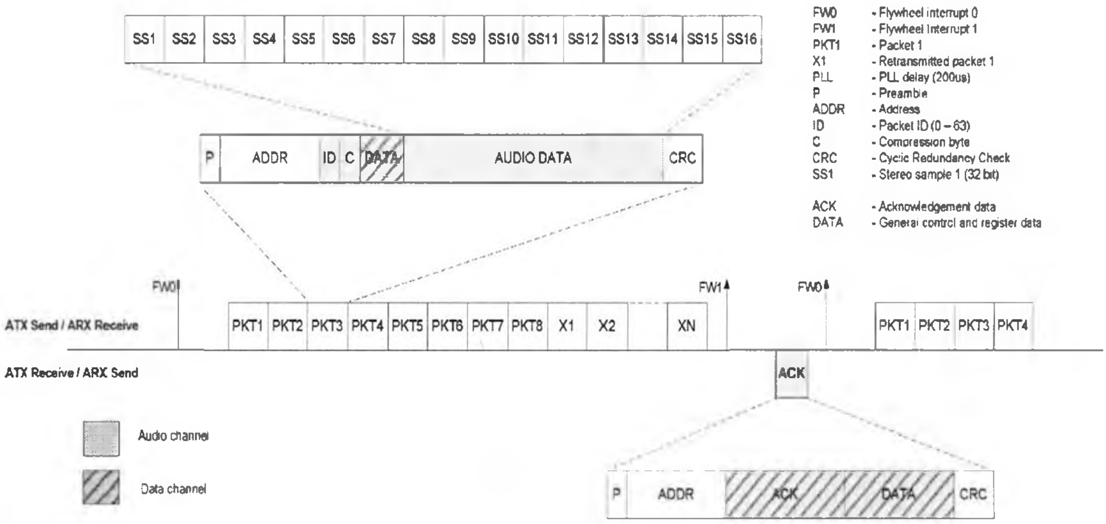

Figure 3-16 nRF24Z1 Data Frame and Packet Organization [29]

3.8.2 Registers in nRF24Z1

nRF24Z1 has more than 50 control and status registers. In our design, the registers are accessed by MCU via the slave interface (SPI). The registers are organized functionally into 7 groups; ATX, Link and ARX control and status, Data link and Test registers. All registers are present both in audio transmitter and audio receiver. The initial values of all registers were read from MCU immediately after power up in our project.

3.8.3 nRF24Z1 Schematics in Transmitter and Receiver

The schematics are shown in Figure 3-17 and Figure 3-18. There are few peripheral components around nRF24Z1. The circuits of transmitter and receiver are similar except that in receiver the Pin MODE connects to GND.

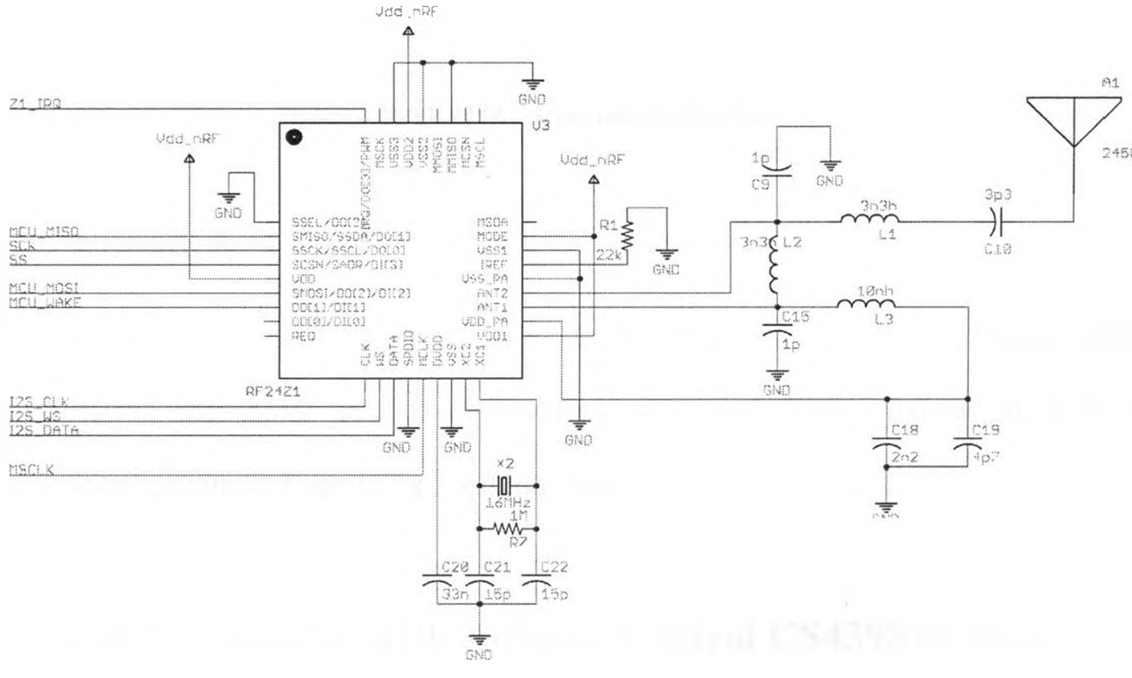

Figure 3-17 nRF24Z1 Schematic in Transmitter

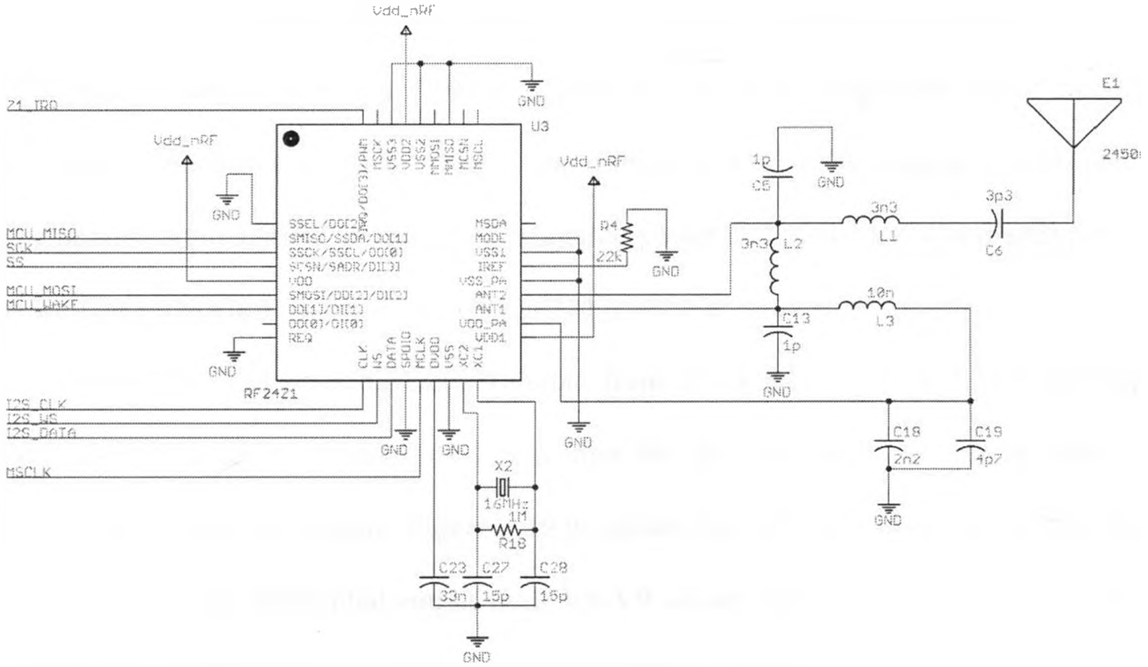

Figure 3-18 nRF24Z1 Schematic in Receiver

3.9 Antennas

The antenna plays an important role in RF communication. So we chose Fractus FR05-S1-N-0-102 chip SMD antenna on the transmitter and receiver boards. It is Omni directional pattern and size is 7 x 3 x 2 mm [30].

3.10 D/A Converter with Volume Control CS4398 in Receiver

The requirements for the D/A converter in wireless system are: (a) ability to playback on two independent channels at sampling rates of 44.1 kHz per channel and 16 bit resolution per sample; (b) Volume Control with less than 1 dB Step Size; (c) Attenuation level at least 100dB. The Cirrus Logic, CS4398, meets all of the requirements. The CS4398 is a complete stereo 24 bit/192 kHz digital-to-analog system. This D/A system includes half dB step size volume control, selectable digital interpolation filters. The CS4398 accepts PCM data at sample rates from 32 kHz to 216 kHz, and delivers excellent sound quality. The output impedance is 118 Ω typically and minimum AC-load Resistance is 1000 ohm. The power supply current is 25mA for 5v analog power and 18mA for 3.3v digital power as well as 1.5 mA for 5V reference voltage [31].

Since the full scale differential output from CS4398 is 1.34*Va=1.34*5=6.7Vpp [31] and the MSB of SDATA of I2S is sign bit, the maximum differential level is 6.7/2=3.35 Vpp in our system. Figure 3-19 illustrates the differential pin output value V8 and V9 Versus the differential output value V8-V9 whose Vpp=1.675+1.675=3.35V. We can find the output from every differential pin is 0.8375V peak.

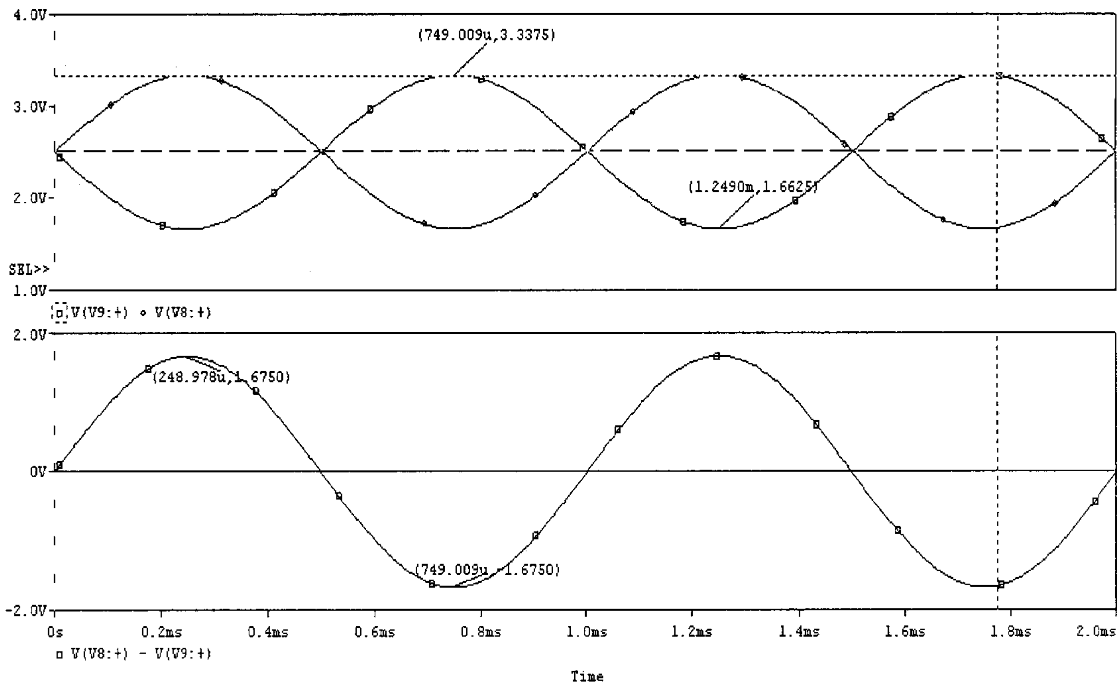

Figure 3-19 Differential Output Illustration

3.10.1 Access Control/Status Registers through Control Port

The control port has two formats: SPI and I2C, with the CS4398 operating as a slave device. If I2C operation is desired, AD0/CS should be tied to VLC or GND. In our design, I2C was employed.

In our design, Pins AD0 and AD1 formed the partial chip address and were tied to GND. The upper five bits of the 7-bit address field were 10011. Therefore, the upper seven address was 1001100. We only used writing function. Figure 3-21 shows the schematic of CS4398.

CS 4398 has nine 8-bits wide control registers. To write to the CS4398, initiate a START condition of the bus (see Figure 3-20). Next, send the chip address 1001100. The eighth bit of the address byte is the R/W bit (low for a write). The next byte is the Memory Address Pointer, MAP, which selects the register to be read or written. The MAP is then followed by the data to be written [31].

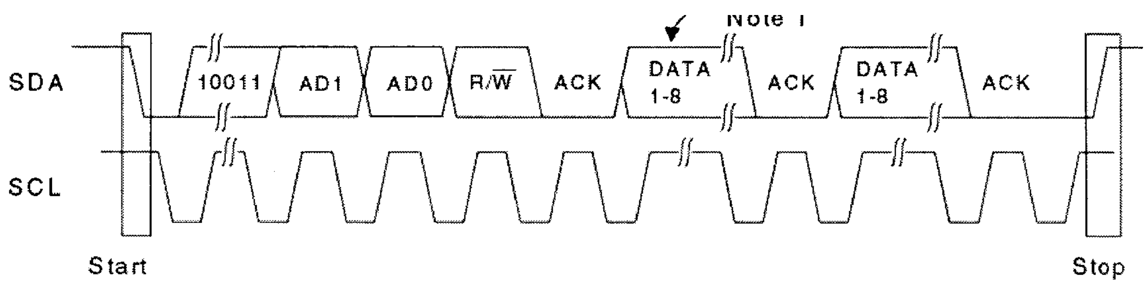

Figure 3-20 I2C Signal Format [31]

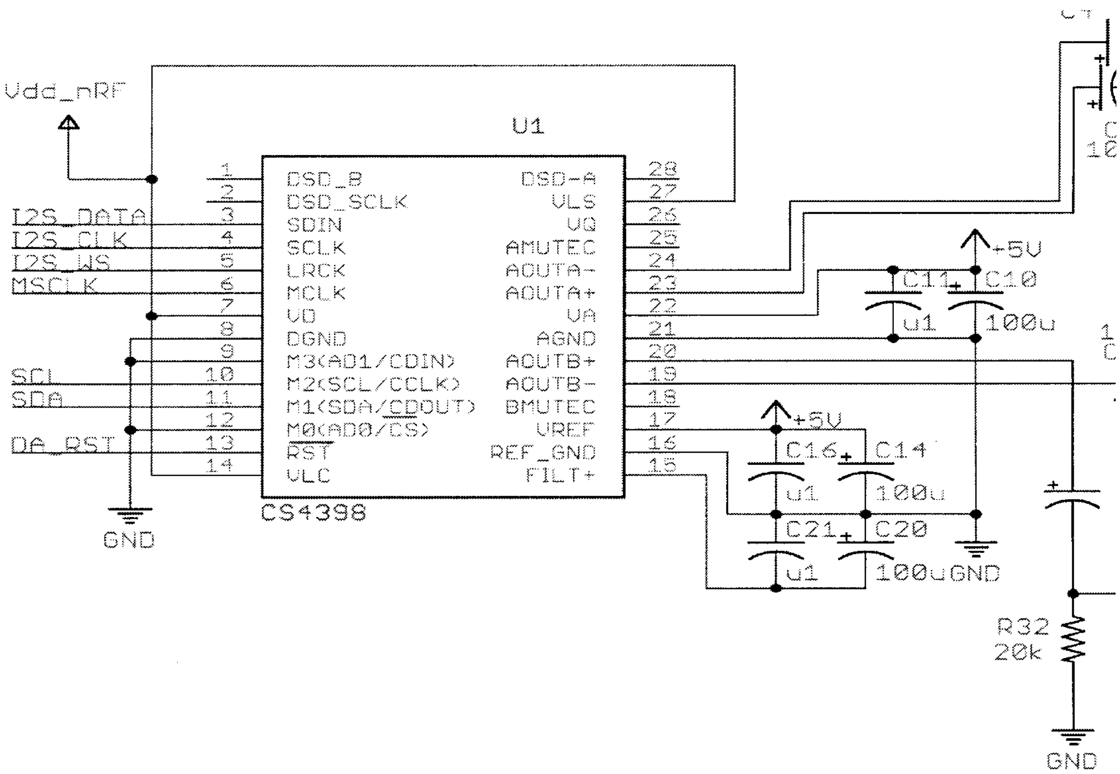

Figure 3-21 CS4398 Schematic

3.10.2 Volume Control

The Digital Volume Control registers allow independent control of the signal levels in 1/2 dB increments from 0 to -127.5 dB. Volume settings are decoded as shown in Table 3.1.

Binary Code	Decimal Value	Volume Setting
00000000	0	0 dB
00000001	1	-0.5 dB
00000110	6	-3.0 dB
11111111	255	-127.5 dB

Table 3-1 Examples Digital Volume Setting of CS4398

3.11 DAC Output Amplifier for CS4398 and Output Level Estimation

In order to achieve low distortion audio signal, a filter and differential to single-ended converter recommended by Cirrus Logic was used to remove the high frequency noise present on the output pins, as well as to provide differential-to-single-ended conversion as shown in Figure 3-22.

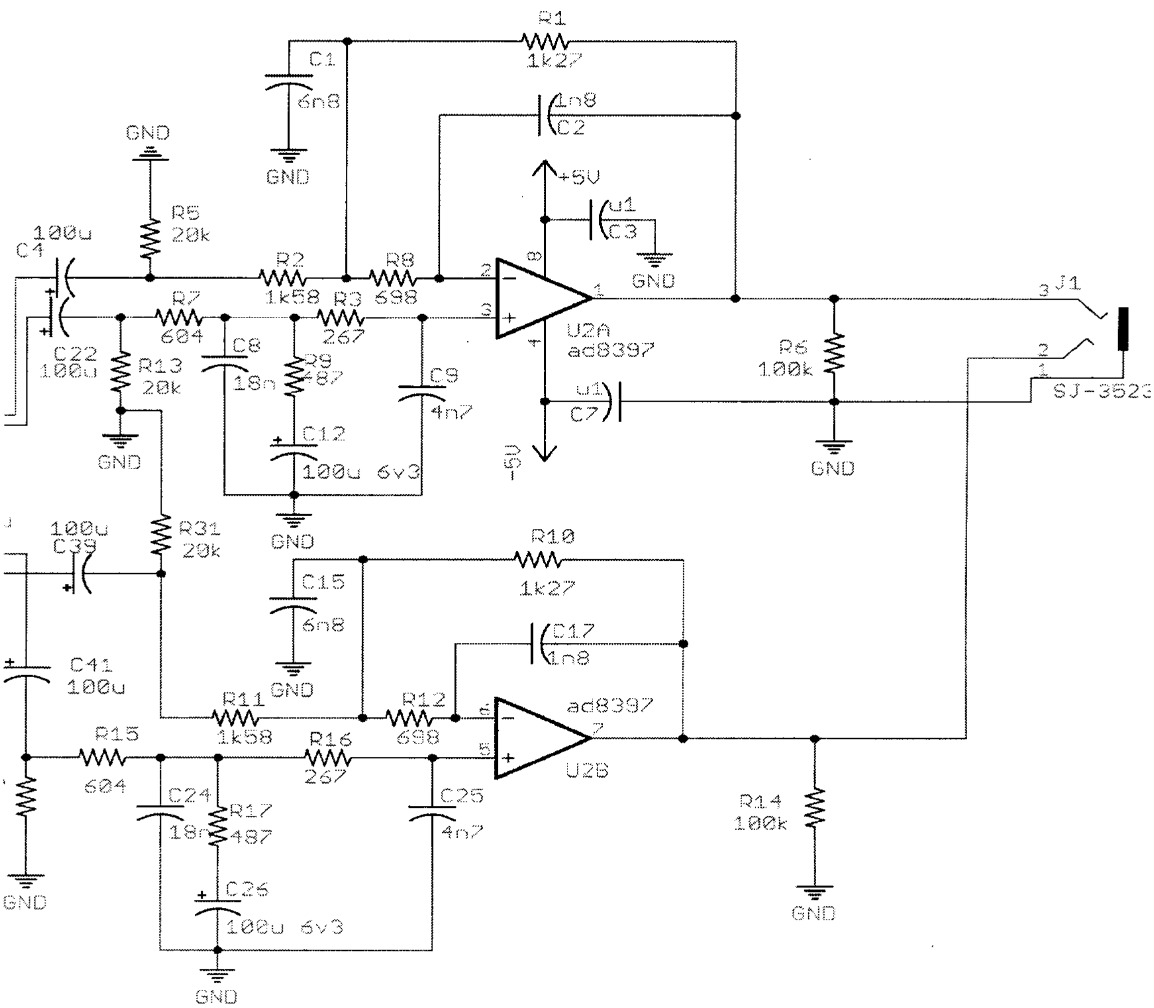

Figure 3-22 AD8397 Schematic

Considering the output load is a 40 Ω headphone, we chose AD8397 as the OP amp. The low distortion, high output current, and wide output dynamic range make the AD8397 ideal for applications that require a large signal swing into a heavy load. Figure 3-24 and Figure 3-25 show the AC sweep output and impedance results from PSpice 15.7.

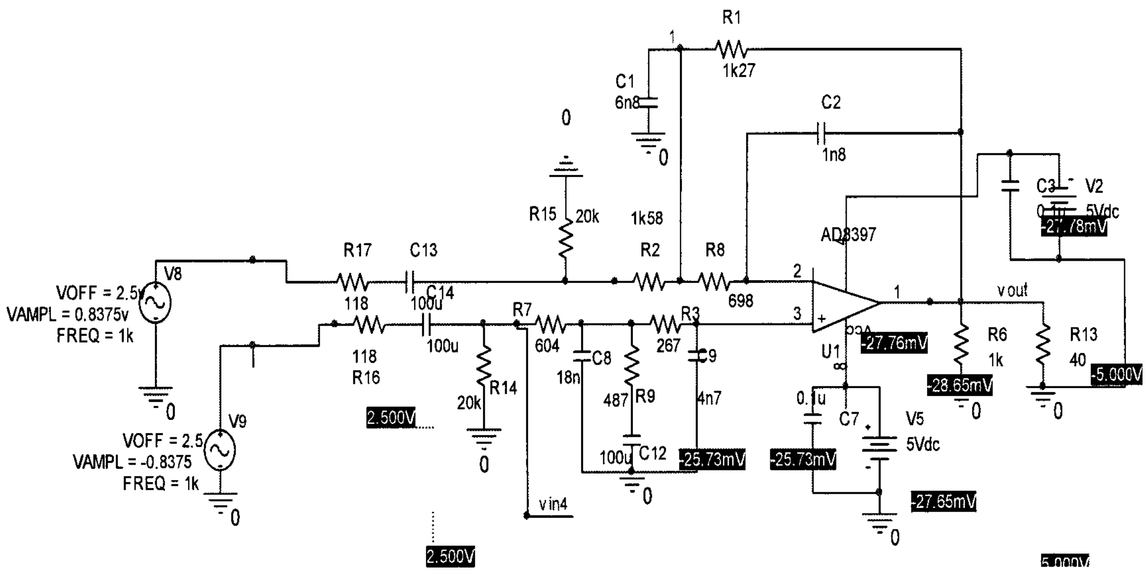

Figure 3-23 Schematic of DAC Output Amplifier for Simulation

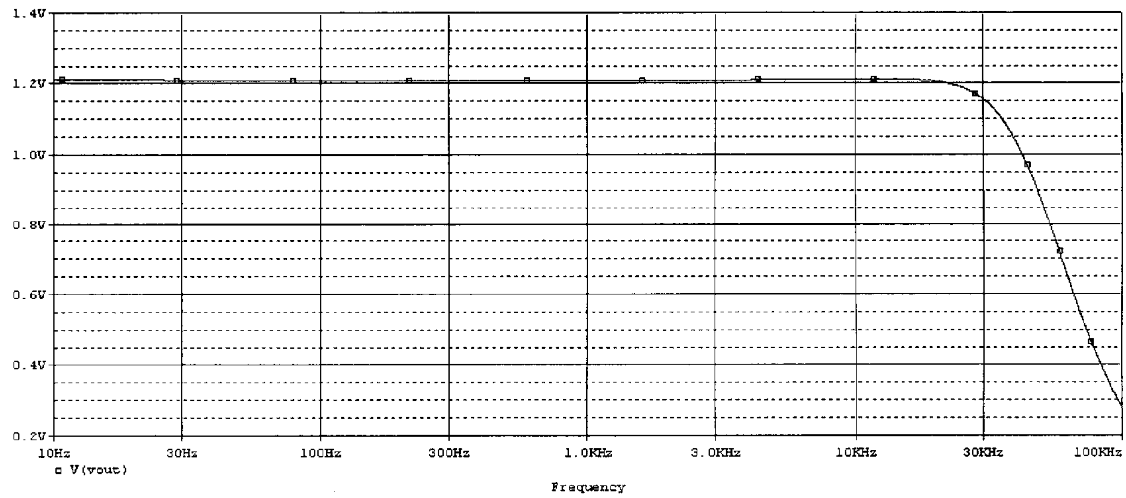

Figure 3-24 Simulation Result of Frequency Response

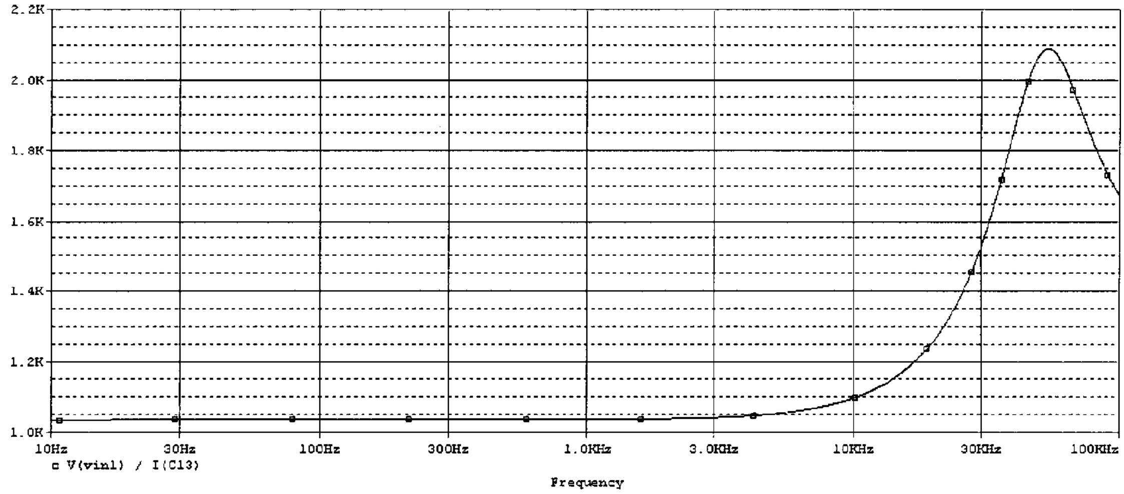

Figure 3-25 Simulation Result of input impedance

From the simulation results, we can find the low-pass filter is very flat from 0-20kHz and the impedance of the amplifier is larger than 1.0k. Since the output from CS4398 is 0.8375Vp, the maximum output from amplifier AD8397 is 1.2*0.7=0.84Vrms. The headphone which we use is the HDA 200 which generates 108.5 dB of SPL (Sound Pressure Level) at 1 kHz, 0.5Vrms [27]. The design consequently meets the hearing test signal level requirement.

3.12 Total Current Estimation, Power Supply and Charging Circuit Schematics

In the transmitter, the Mega48 and nRF24Z1 work at 3.3v. Mega48 active current is 3mA when working at 8MHz [24]. The total current

Itotal=Imega48+I24z1=3+17=20mA.

Hence we chose linear voltage regulator LM3480 which provides 100mA Max [32]. Since the transmitter is powered by USB port, we had to calculate the current consumption. The total current in transmitter

$$I_{transmitter}=I_{cm108}+I_{mega48}+I_{24z1}=27+3+17= 47mA$$

Again, since the USB protocol usually provides at least 500mA, the transmitter meets the current requirement.

In receiver, we assumed the voltage converter works ideally, i.e. the efficiency is 100%. So the 5v and -5v current summation for providing power to load is 0.84Vrms*0.84Vrms/40/5 = 3.5 mA Max

Total receiver current from 5v

$$I_{receiver}=I_{cs4398}+I_{24z1}+I_{mega48}+I_{ad8397}= (25+18+1.5)+23+3+(3.5+8.5+8.5) = 91\ mA$$

plus practical loss. Hence, we chose a 7.2v 1Ah lithium battery, with the charging and protection circuit designed as shown in Figure 3-26.

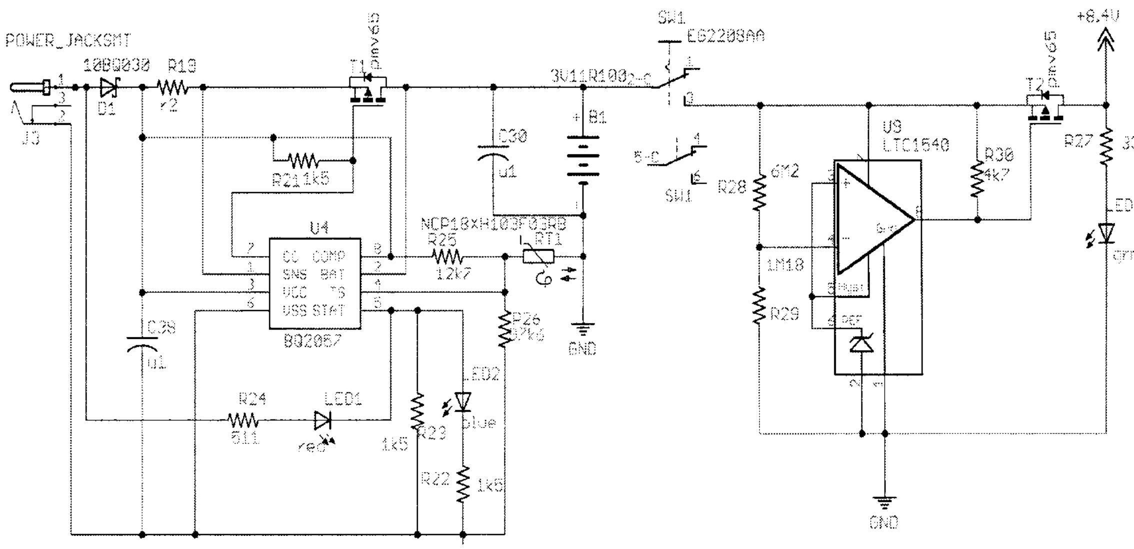

Figure 3-26 Power Supply and Charging Schematic in Receiver

3.13 Printed Circuit Board (PCB) layout

A PCB is used for electronic components connection and mechanical support. Since there are analog, digital and RF signals on the boards, a considerable amount of time was spent to do layout carefully with minor modifications along the way during design.

3.13.1 PCB Layout Implementation

The tool we used for our design was the Altium Designer 6.6 from Altium Company, which is shown in Figure 3-27.

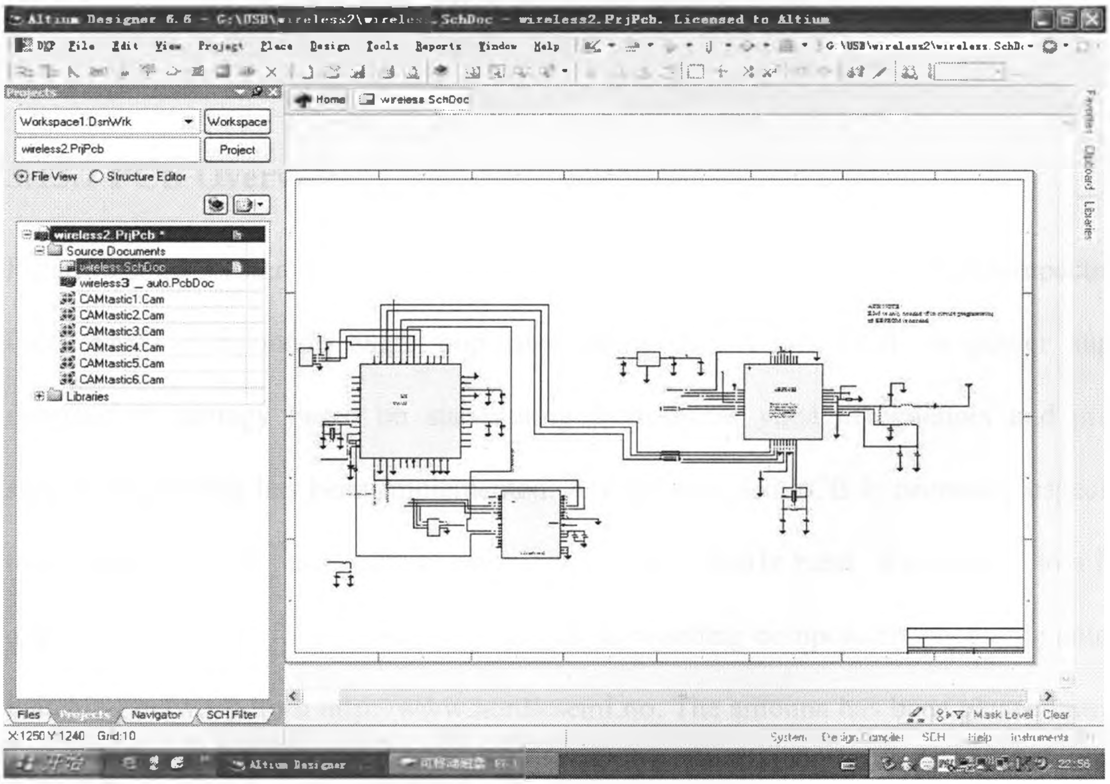

Figure 3-27 Screenshot of Altium Designer 6.6

Firstly, in order to draw circuit schematics, component symbols and PCB footprints were created if they were not in Altium library. Once all of the required parts were added to the library, they were placed in the schematic and connected by wires. After that, the schematic of the design was created. Then we compiled the project to check for errors before converting the schematic into a blank PCB document. Each component was then on a PCB file if no errors. After component placement, we used automatic and manual routing to place wires between each electrical node. Clearance was set in the design according to the PCB design rules and PCB manufacturers' recommendations. Separate ground was created for the analog and digital components to reduce digital noise in the analog section.

3.13.2 PCB Overview

Figure 3-28 3-29 and 3-30 show the PCBs designed for our system. For compactness, 0603 SMD components were populated on a double-side PCB. A power supply distribution strategy based on star-routing from linear voltage regulators and proper supply decoupling has been implemented. A well-designed PCB is necessary especially to achieve good RF performance, especially for the 2.4GHz band. We referred to a fully qualified RF-layout for the nRF24Z1 and its surrounding components, including antenna matching network from http://www.nordicsemi.no. The antenna has been placed onto the ATX and ARX boards according to the recommendations given in the Fractus antenna "User Manual" [30]. The nRF24Z1 is a two-way package based radio, meaning it will constantly switch between transmit-receive-transmit-receive and so on. The current drawn will be different, which may give rise to voltage ripple on the power supply. Therefore, the nRF24Z1 has its own power supply line from the supply source. The receiver is larger than transmitter because more components were used in receiver such as the filter, the charging circuit and the negative voltage generator. The physical dimension for the PCB board is 155mm x 102 mm for wired system and 45mmx30mm, 77mmx49mm for wireless system.

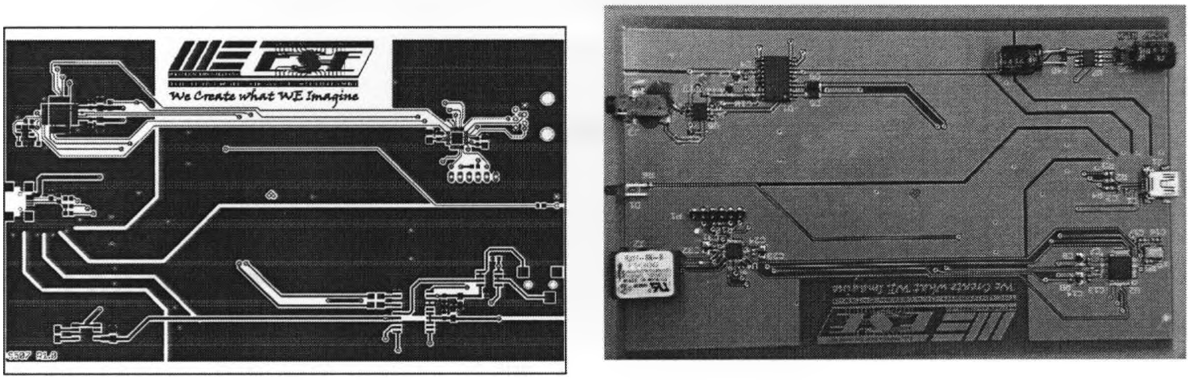

Figure 3-28 PCB of Wired System and PCB after Population

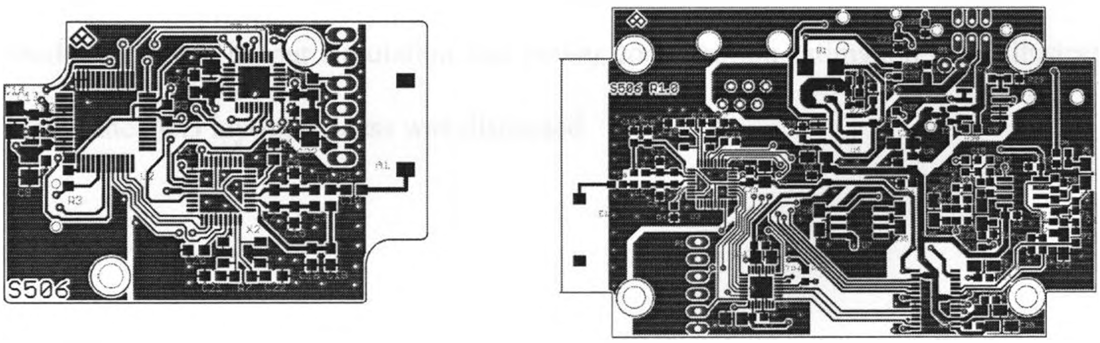

Figure 3-29 PCBs of Wireless System

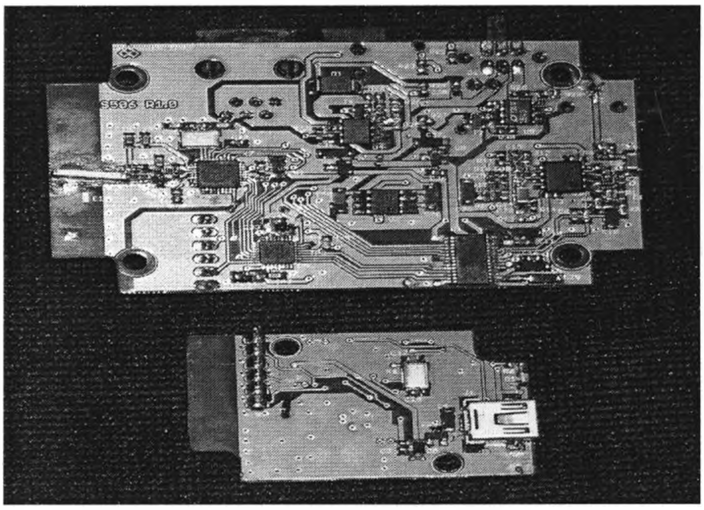

Figure 3-30 The Final Wireless PCBs after Population

3.14 Summary

In this chapter, hardware designs of the wired and the wireless psychoacoustic testing system were presented. The system block diagrams were discussed. Core chips and schematics such as CM108, nRF24Z1, Mega8, mega48, LM1973 and CS4398, were introduced. Then, output simulation and power consumption estimation were illustrated. Finally, the PCB layout process was discussed.

Chapter 4

Firmware Development

Firmware development is another important section in the thesis. In this chapter, The MCU source code development in wired and wireless systems will be presented. The algorithms include polling loop and interrupt response as well as FSM (Finite state machine). These algorithms make the code reliable, readable and easy to debug. We will discuss wired system firmware firstly since it is more straightforward and then the wireless system. The firmware was written in C using ICCv7 for AVR and programming tool was BASCOM AVR.

4.1 Firmware Development of Wired System

The firmware of wired system has two major goals to fulfill. The first is to decode the sound attenuation data from CM108. The second is to ensure that button status data are sent to the host quickly so that the display on the host appears to be real time. The following sections give the design approach in flowcharts.

4.1.1 Prototype: Main

Description:

1. At power-up, internal ports and interrupt configuration registers on Mega8 are initialized.
2. The firmware runs a polling loop.

3. Mega8 detects audio attenuation data firstly. If any data come, INT0 will be triggered and a flag will be set, then a subroutine executes to retrieve the attenuation signal. Next, the data are sent to LM1973 from Mega8 via SPI.
4. After that, Mega8 detects button status. If buttons pressed, these button data will be sent to CM108 by GPIO.

Figure 4-1 shows the main routine flowchart.

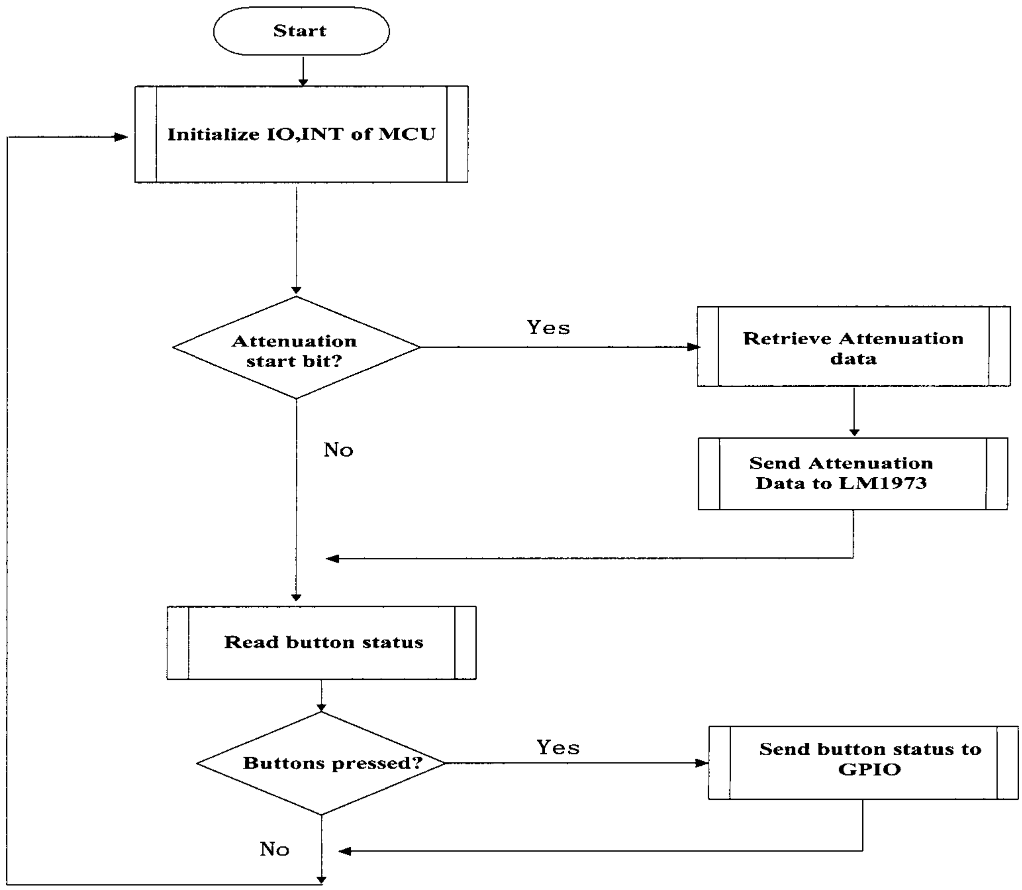

Figure 4-1 Main Routine of Wired System

4.1.2 Prototype: Initialize IO and INT of MCU

Description: The goal is to initialize Mega8 after power on reset. This routine does the following operations:

1. Set PortB, PortC and PortD directions
2. Set Pull-up resistors
3. Set interrupt configuration registers. Enables INT0 and INT1 rising edge interrupt.

Figure 4-2 shows the Mega8 initialization.

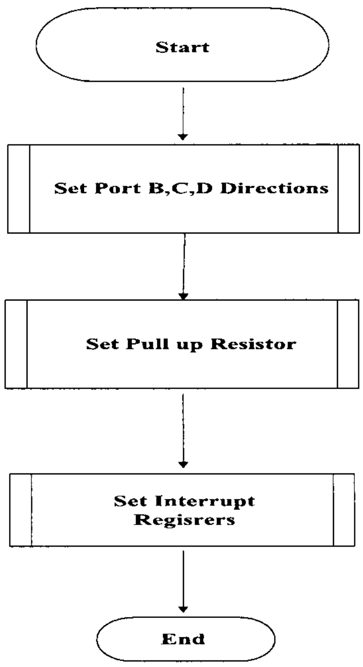

Figure 4-2 Initialize IO and INT of Mega8

4.1.3 Prototype: Retrieve Sound Attenuation Data from CM108

Description: Since USB audio controller (CM108) only has GPIO pins, we had to adopt certain method to decode channel and attenuation data from GPIO1, GPIO2 on CM108. The protocol is simplified from I2C protocol. The format is shown in Figure 4-3:

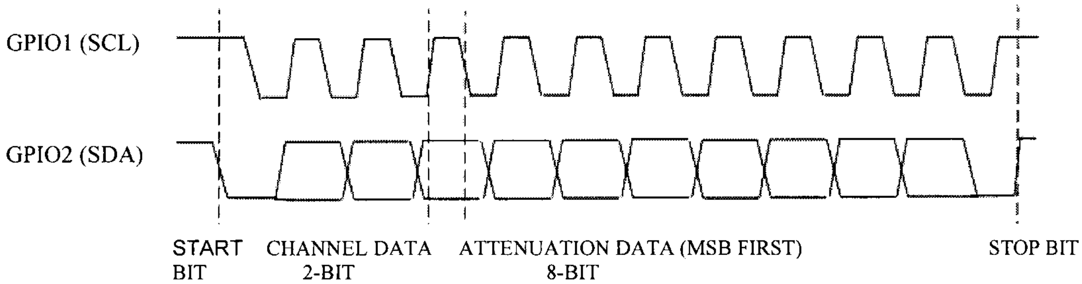

Figure 4-3 Sound Attenuation Data Format

For retrieving sound attenuation data from CM108, firstly, MCU determines the bit number it has received. The total attenuation signal data length is 2(channel data) +8(attenuation data) =10 bits and this number starts from 0 in initialization. If the number is less than 10, the MCU has to run in a loop to attain all of the ten bits. In the loop, the MCU waits for the rising edge of SCL, then shifts the received content 1 bit left, puts the new bit in the LSB (Least Significant Bit). After ten times receptions, the whole sound attenuation signal data are attained. For quick and accurate response to sound level data, INT0 and INT1 are used to detect rising edges of SDA and SCL. Their service routines can set corresponding flag in main routine. The process can be seen from Figure 4-4.

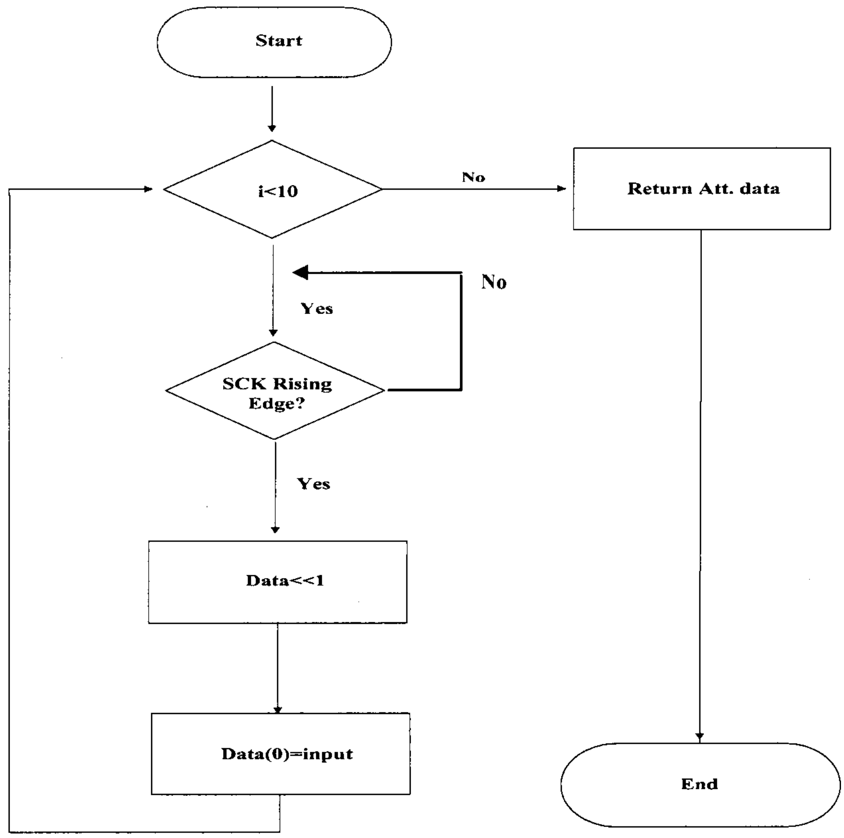

Figure 4-4 Retrieve Sound Attenuation Data

4.1.4 Prototype: Detect and Send Button Status

As shown in Figure 4-5, when a button is pressed or released, the contacts of a switch bounce in a short time, resulting in a jagged signal. When this signal is sent to MCU, the MCU which runs in high speed can recognize this as multiple button presses, causing the application software to act as if multiple, very fast button presses have occurred. Since a button is normally considered to be debounced if it does not change state for 10 ms or longer, MCU polls the switch line in 10 ms until the switch line stays at the same level to avoid this problem.

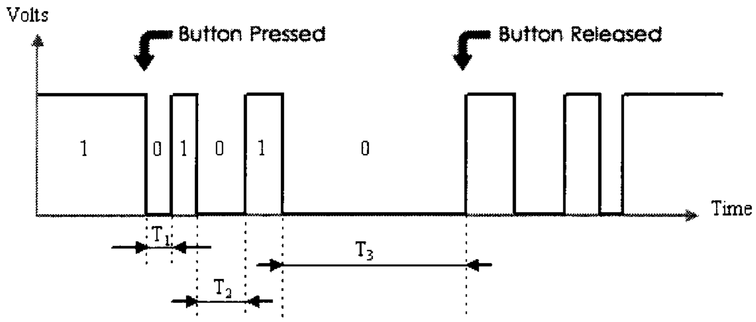

Figure 4-5 Waveform of Button Bounce

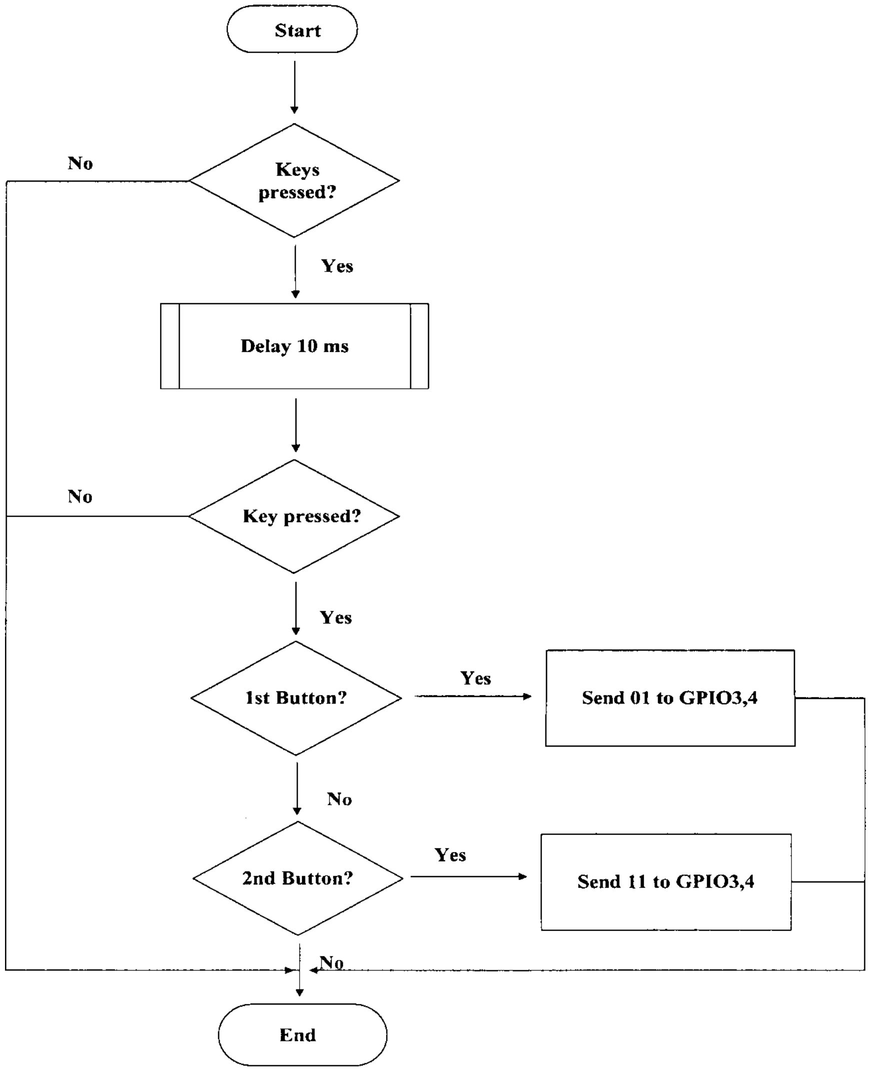

Figure 4-6 Flowchart of Detecting and Sending Button Status

Figure 4-6 shows the flow chart to detect and send button status. GPIO3=0 and GPIO4=1 means button 1 pressed as well as GPIO3=1 and GPIO4=1 means button2 is pressed. The GPIO3 and GPIO4 signal are stable for a short time for the host polls these data through USB.

4.2 Firmware Development of Transmitter in Wireless System

The wireless system includes a transmitter and a receiver. Mega48 MCU in the transmitter achieves three major goals. The first is to decode the sound level data from CM108. The second is to ensure that button status data is sent to the host quickly and the final goal is to ensure the attenuation data sending to receiver immediately. The firmware consists of several routines and will be described as bellows.

4.2.1 Prototype: Main

Description:

1. At power-up, internal ports, interrupt configuration registers and UART configuration registers on Mega48 are initialized. This routine is similar to the wired system.
2. The user function Init_z1 is called to initialize wireless chip nRF24Z1.
3. An endless loop starts. The firmware detects debugging data firstly. If any data come, corresponding commands are executed. Because it is for debugging purpose, this part is not included in final version.

4. INT0 interrupt service routine which is similar to the wired system executes if sound attenuation data has arrived from CM108. To feed these data to nRF24Z1 which transmits them to receiver by RF, the firmware uses RXBUF (0x60, 0x61) to transfer channel data (1 byte) and attenuation data (1byte) one way at a time. RXWCNT (0x71) and RXRCNT (0x0x72) is set to the number of bytes to transfer and which way. The RXDCMD (0x0x70) is set to 0x8E.
5. The firmware reads corresponding registers if buttons status data come from receiver. PCINT0 is used to respond this event. Then buttons status is sent to CM108 through GPIO if buttons are pressed.

Figure 4-7 shows the flowchart of main routine.

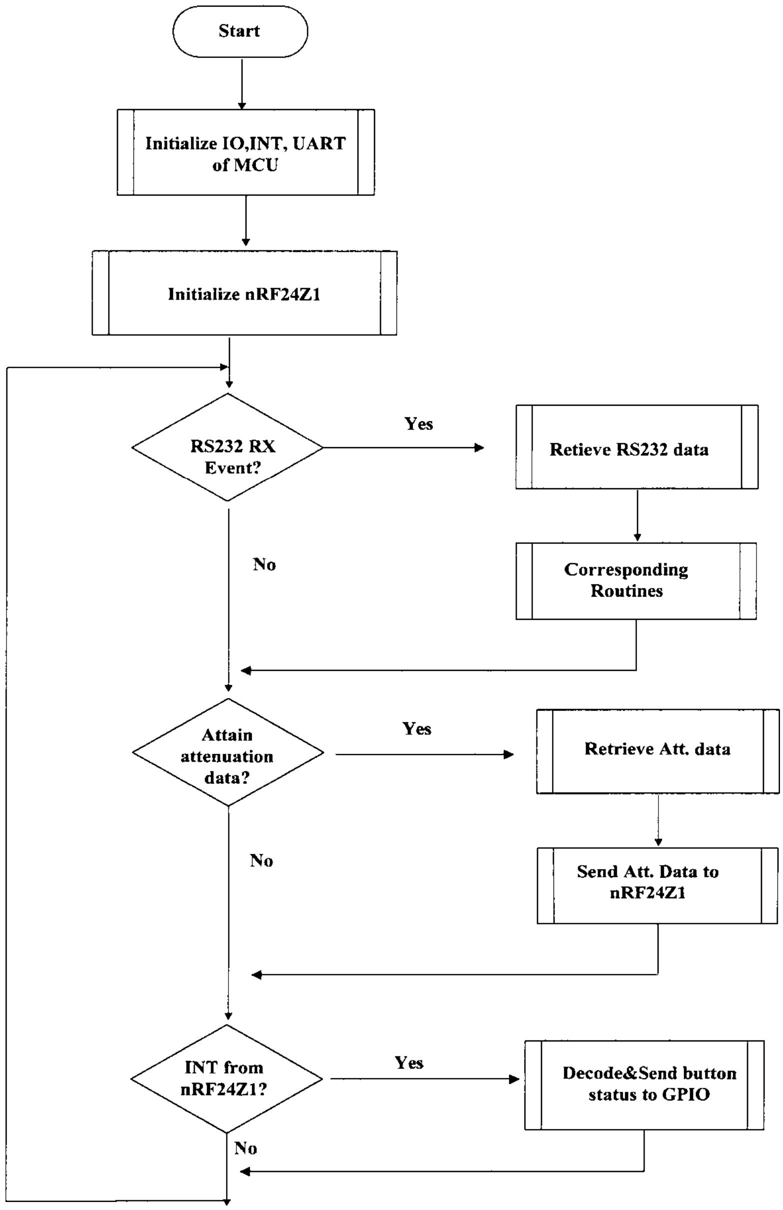

Figure 4-7 Main Flowchart of Transmitter

4.2.2 Prototype: Initialize nRF24Z1

This routine shown in Figure 4-8 does the following operations:

1. Set I2S audio data speed as hardware automatically detection.
2. Set an address for the TX which is identical to RX

3. Set Hopping frequencies to ensure hopping operation

4. Set RF power to 0dBm

5. Set interrupt configuration register to enable remote transfer done interrupt

6. Enable transceiver to work.

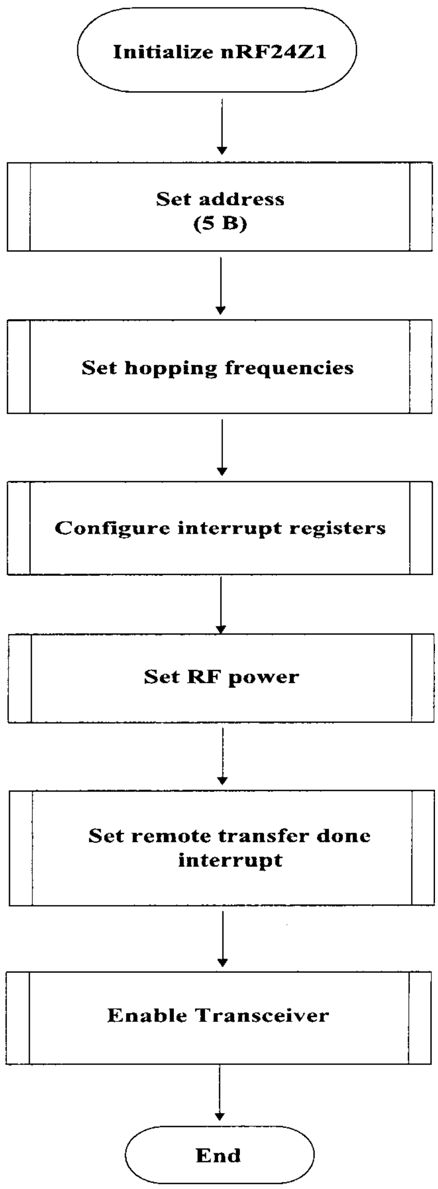

Figure 4-8 Initialize nRF24Z1

4.2.3 Prototype: Retrieve UART Data for Debugging

Description: Although in the final version of project, both the hardware and code are removed, the debugging routine is very important and useful during the firmware developing. As mentioned in the last chapter, nRF24Z1 has more than fifty control and status registers. These registers can be accessed by MCU via SPI. It is more convenient for debugging if we are able to read and write the content of these registers from PC side using some serial communication software such as "Access Port". Figure 4-10 shows the screenshot of this software.

According to the SPI slave interface of nRF24Z1, the first byte of the SPI transaction specifies the register address and whether it is a read or a write access. The seven least significant bits in the first byte is the nRF24Z1 register address, while the most significant bit is the read/write indicator (read=1, write=0) [29], see Table 4-1.

B7	B6	B5	B4	B3	B2	B1	B0
R/W	Register address						

Table 4-1 SPI Command Byte Encoding [29]

In write transaction, the next byte on SMOSI will be put into the register with the address specified in the first byte. Writing additional bytes will increment the register address automatically [29].

In read transaction, the next byte on SMISO will be the contents of the register with address as specified in the first byte. Reading more bytes will increment the register address automatically [29].

To simplify the debugging code, we adopted the same data format which is taken to access nRF24Z1 by MCU. These data are sent from PC. Firstly, PC sends address if we need the content in the address. Then nRF24Z1 sends back the address and content through RS-232. If we write data to an address in nRF24Z1, we send 8 bit address as Table 4-1 followed by the 8-bit data. The nRF24Z1 returns the address and data to PC after writing the data in address. However, there are some issues we have to solve. For example, how to determine the data received in MCU from RS232 whose MSB equals to "1" is the first byte to read or the second byte to write. In the former firmware version, we set several flags to indicate the different situations in transaction but got errors occasionally. Later, we used FSM (Finite State Machine) to design this routine which runs correctly.

Figure 4-9 shows the FSM flow chart:

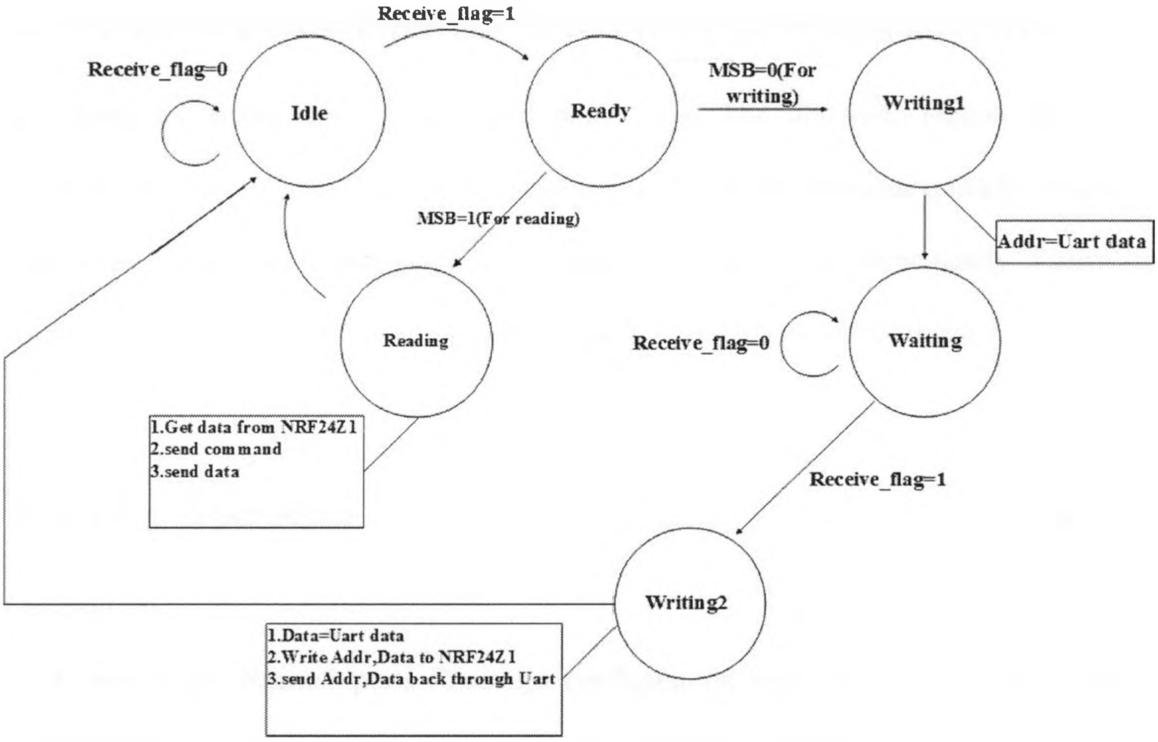

Figure 4-9 FSM for UART Data

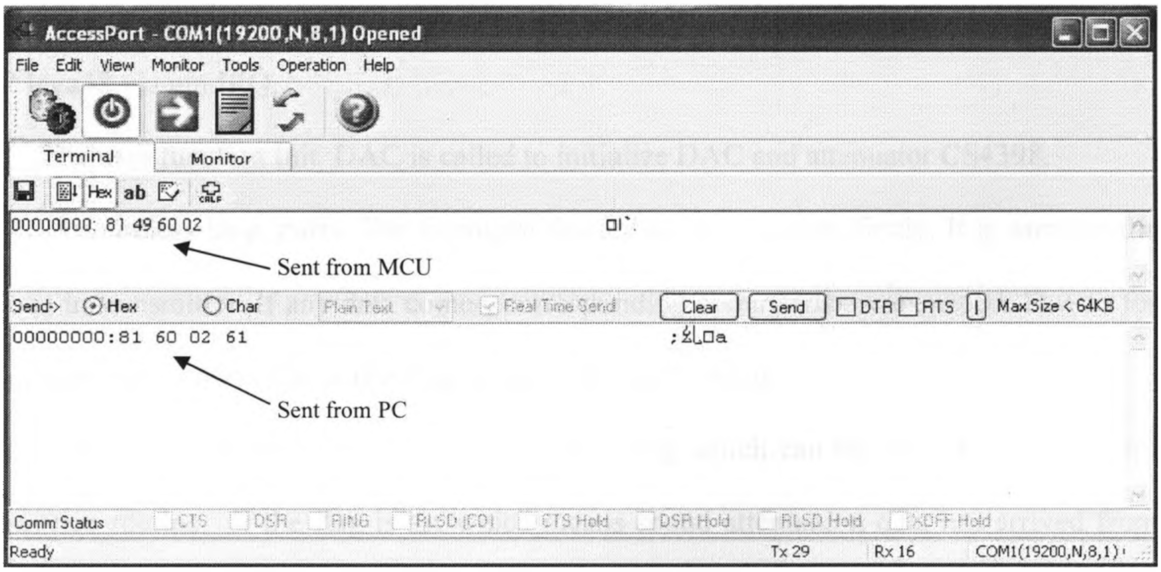

Figure 4-10 Screenshot of AccessPort Software

4.3 Firmware Development of Receiver in Wireless System

The firmware in the receiver has three major tasks. The first is to receive the sound attenuation data from nRF24Z1. The second is to detect button status quickly. The final goal is to ensure the button status data sending to transmitter immediately. Firmware routines descriptions and flowcharts will be given in the following sections.

4.3.1 Prototype: Main

Description:

1. At power-up, internal ports, interrupt configuration registers, UART configuration registers as well as I2C configuration registers on Mega48 are initialized,

2. The user function Init_Z1_RX is called to initialize wireless chip nRF24Z1. This routine is similar to transmitter. The nRF24Z1 is configured to deliver interrupt to Mega48 via pin IRQ.

3. The user function Init_DAC is called to initialize DAC and attenuator CS4398.

4. An endless loop starts. The firmware detects debugging data firstly. It is same to the one in transmitter. If any data comes, corresponding commands are executed. Due to for debugging purpose, this part is not included in final version.

5. The firmware begins to check the interrupt flag which can be set in INT 0 interrupt service routine. If the flag is set which means sound attenuation data has arrived from transmitter, The firmware then retrieves these data and feed to CS4398 .

6. The firmware polls corresponding local IO ports to detect buttons status. If buttons are pressed, then buttons status is sent to nRF24z1 through SPI bus.

Figure 4-11 shows the main routine flowchart.

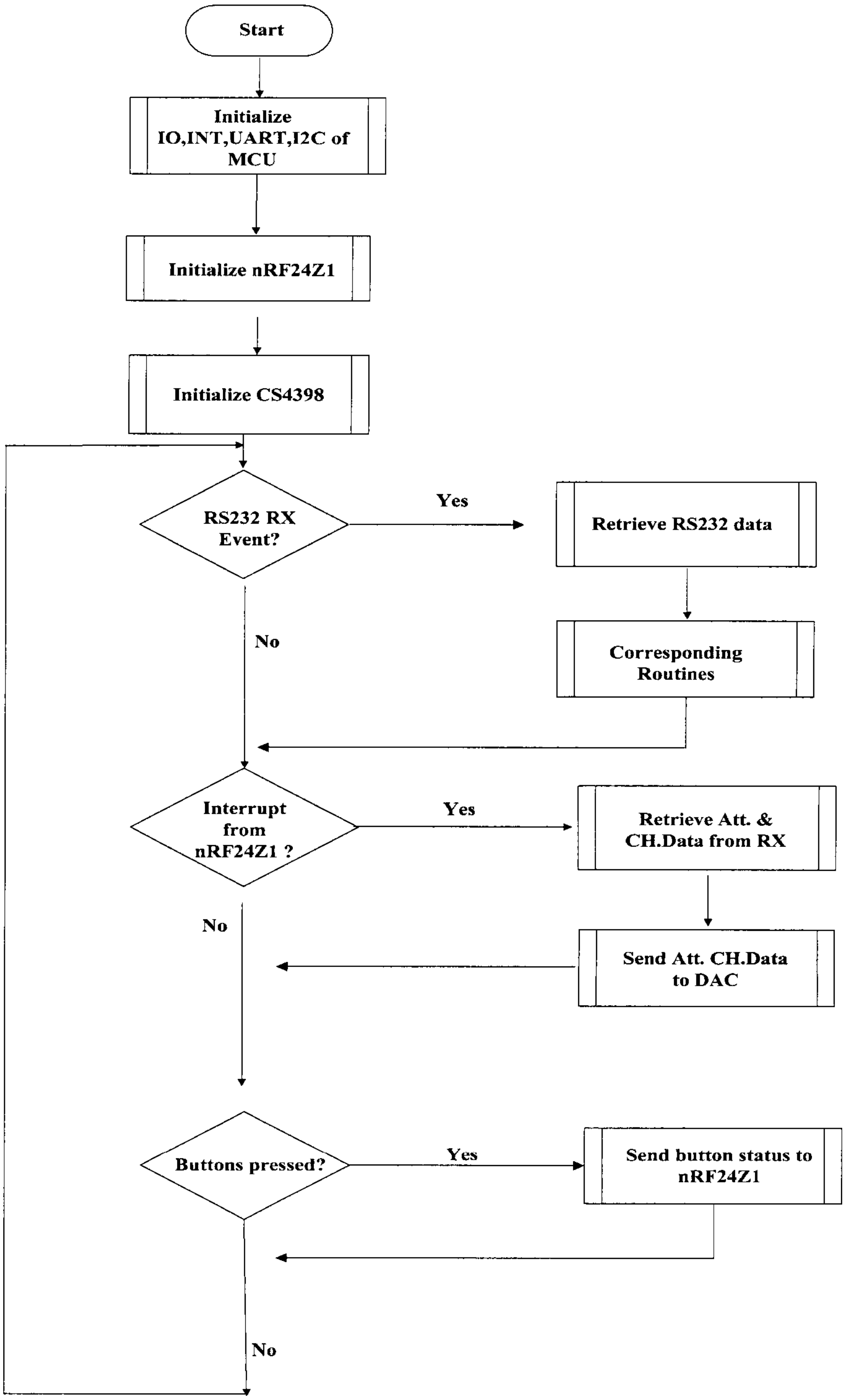

Figure 4-11 Main Routine Flowchart of Receiver

4.3.2 Prototype: Initialize CS4398

Description: To initialize DAC chip CS4398 through I2C bus after power on reset. This routine does the following operations as shown in Figure 4-12:

1. Configure Misc.Control register to enable access to control port.
2. Set I2S data format up to 24 bit.
3. Disable Power down Mode for normal operation.
4. Mute both left and right channels.

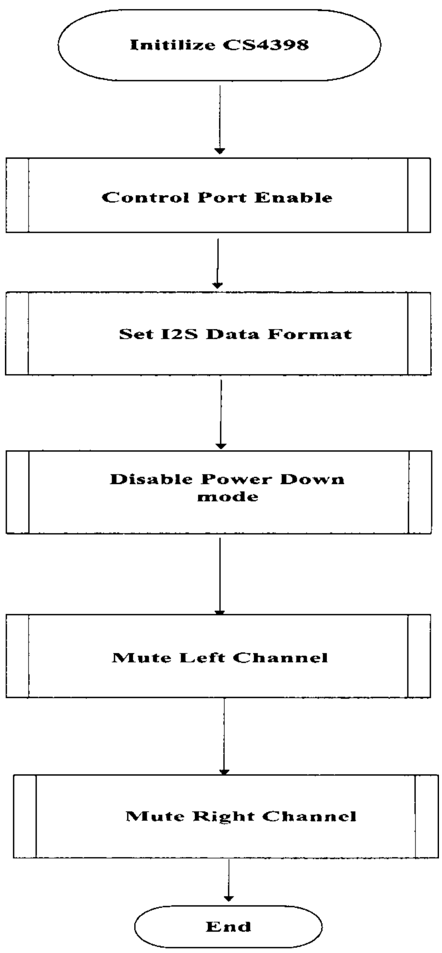

Figure 4-12 Initialize CS4398

4.3.3 Prototype: Retrieve Attenuation Data and Send to CS4398

Description: The firmware checks the interrupt flag which can be set in INT 0 interrupt service routine. The pin IRQ of nRF24Z1 can trigger this interrupt. If so, MCU then reads interrupt status register in nRF24Z1. If bit 3 which is RXPIO register value changes status, the flag is set. The firmware reads channel and attenuation data from register 0xe0 and 0xe1. After that, these data are sent to DAC through I2C. The final step is to clear the interrupt flags in both mega48 and nRF24Z1 to wait for next interrupt event.

The flowchart shows the operation process in Figure 4-13.

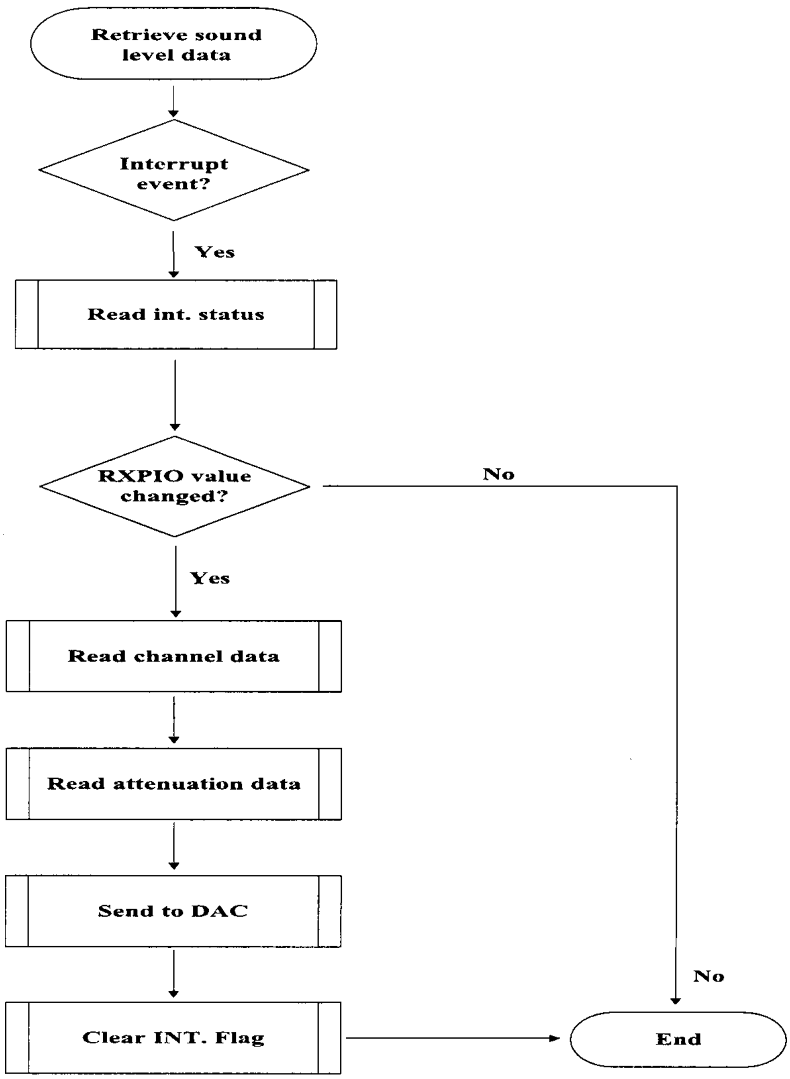

Figure 4-13 Flowchart of Retrieving and Sending Attenuation Data

4.4 Summary

This chapter discussed the firmware development procedure of our system. Both wired and wireless system are presented. Some routines in these two systems are similar. Core firmware routines descriptions and flowcharts have been discussed.

Chapter 5

Instrumental and Behavioural Evaluations

The hardware and firmware of the wired and the wireless system are presented in previous chapters. As an example, the finished wireless system is shown in Figures 5-1 and 5-2.

Figure 5-1 Wireless Transmitter and Receiver with Response Buttons

Figure 5-2 Headphones with Receiver and a Handheld PC Running Psychoacoustic Test Software

In this chapter, further validation of the proposed systems is undertaken for evaluation. In addition to RF measurement of the wireless system, the electroacoustic performance of the systems in terms of its frequency response and distortion is investigated. Furthermore, small scale behavioural measurements of frequency discrimination, gap detection, and TMTF (Temporal Modulation Transfer Function) were conducted with a group of normal hearing listeners to further validate the designed psychoacoustic test systems.

5.1 Electrical Characteristics of the Systems

Electrical parameters are essential for our systems, and some of electrical parameters measured with the systems are listed in Table 5-1. Table 5-2 details the audio output of wired and wireless system in RMS voltage with different attenuations when the input is 1 kHz sine wave and the load is HDA200 headphone [27].

Parameter	System	Min.	Typ.	Max.	Units
Supply Voltage	wired		5.0		V
	Wireless transmitter		5.0		
	Wireless receiver	6.0	7.4	8.4	
Power Supply Current	wired	80	90	120	mA
	Wireless transmitter	47	50	53	
	Wireless receiver	94	100	120	

Table 5-1 Electrical Parameters of the Systems

Type	Digital Sine Peak	Attenuator Setting	Measured RMS Voltage	Units
Wired	0.9	0.0	1.197	V
Wireless	0.9	0.0	624	mV
Wired	0.9	7.5	502	mV
Wireless	0.9	2.0	497	mV
Wired	0.9	15.5	198	mV
Wireless	0.9	10.0	195	mV
Wired	0.9	21.0	105	mV
Wireless	0.9	16.0	100	mV

Table 5-2 Audio Output Parameters with Different Attenuations

As reported in Chapter 3, simulations were conducted for wired and wireless system before building the devices. From the simulations, it was estimated that Vrms=1.25v in wired system and Vrms=0.84v in wireless system. The simulation results are close to the actual data in wired system. In wireless receiver, the actual output from CS4398 is 0.7Vp, lower than the data from datasheet.

In addition, the system frequency response was measured with white noise stimulus. A stereo .wav file sampled at 44100 Hz containing white noise samples was played back through the wired psychoacoustic measurement system, with volume controls set to "max" in the host, and the attenuations on the left and right channels set to 0 dB. The output of the wired device was measured using a laptop that contained high quality data acquisition system and spectrum analysis software, SpectraPlus. Figure 5-3 displays the screenshot from the SpectraPlus software showing the results of this experiment. The top graph panel shows the output on the left channel, while the bottom shows the response on the right channel. Furthermore, the red curve was measured at 0 dB attenuation and the yellow curve was measured at 10 dB attenuation on both channels. From this figure, it is evident that the frequency response of the wired system is very flat with white noise stimuli. Similar result was obtained for the frequency response to white-noise of the wireless system.

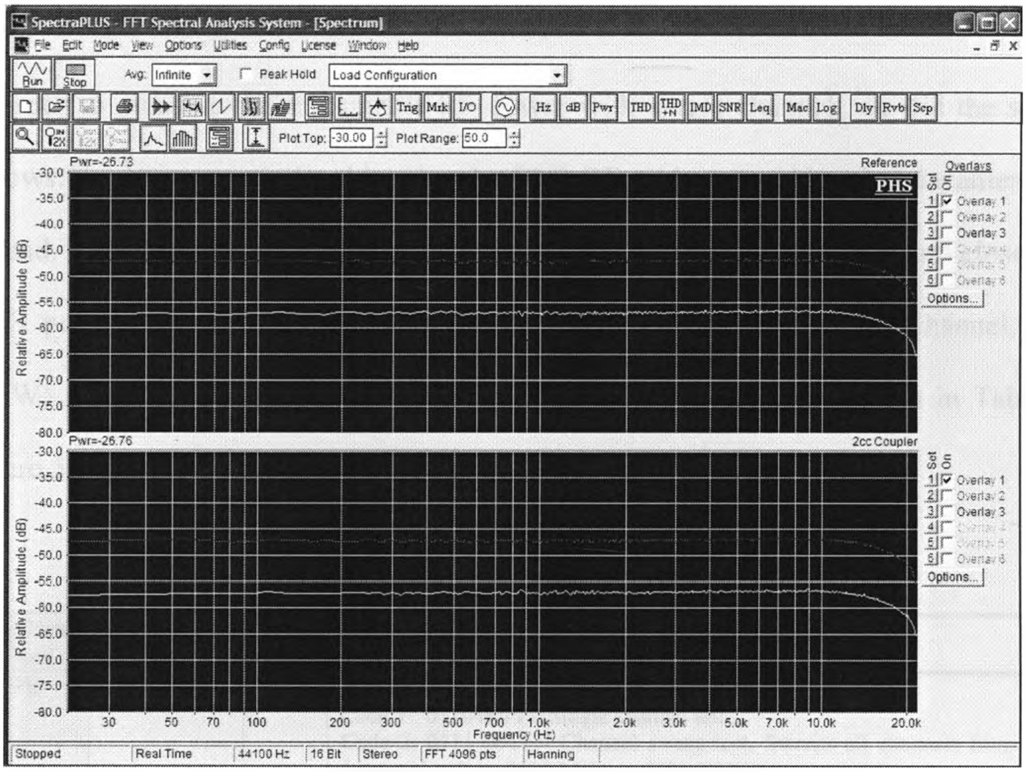

Figure 5-3 SpectraPlus Screenshot of White-noise from Wired System

5.2 RF Power Measurement of Wireless System

In order to test the RF characteristics of our wireless system, we conducted RF power measurements. To put our measurements in perspective, we compared the measurements from our system with those obtained with the Kleer system [19]. Because we did not have RF variable attenuator for the sensitivity measurement, only RF transmission power was measured by Agilent E4404B spectrum analyzer for our project.

5.2.1 Wireless System (Based on nRF24Z1) Measurement

Firstly, we measured the transmitter and receiver RF power from nRF24Z1.

5.2.1.1 Single Channel Measurement Set-up

In order to measure the transmitter RF power with single channel, we did the steps as follows: the antenna was desoldered and a 50 Ω RF cable was soldered to the antenna pad instead. The cable screen was firmly soldered to the board ground plane and close to the 50 Ω point. Next, we programmed the nRF24Z1 to TX mode, single channel, 0dBm (1mW) using transmitter testing firmware. The related register is shown in Table 5-3. Figure 5-4 shows the transmitter measurement set-up.

Address Hex	Register	R/W	Description	
0x7E	TESTREG	W	Test mode register: Code 1: 0110 0011 – Single channel test. Code 2: 0111 0011 – Channel sweep test. Sweeps all channels from frequencies from 2400 MHz to 2480 MHz in steps of 1MHz.	
0x7F	TESTCH	W	Bit	Interpretation
			7	1: TX, 0: RX Initiates the mode described in TESTREG in RX / TX mode.
			6:0	Channel number when TESTREG is set to Code 1 (single channel), number is in 1MHz step relative to 2400MHz

Table 5-3 Test Register of nRF24Z1 [29]

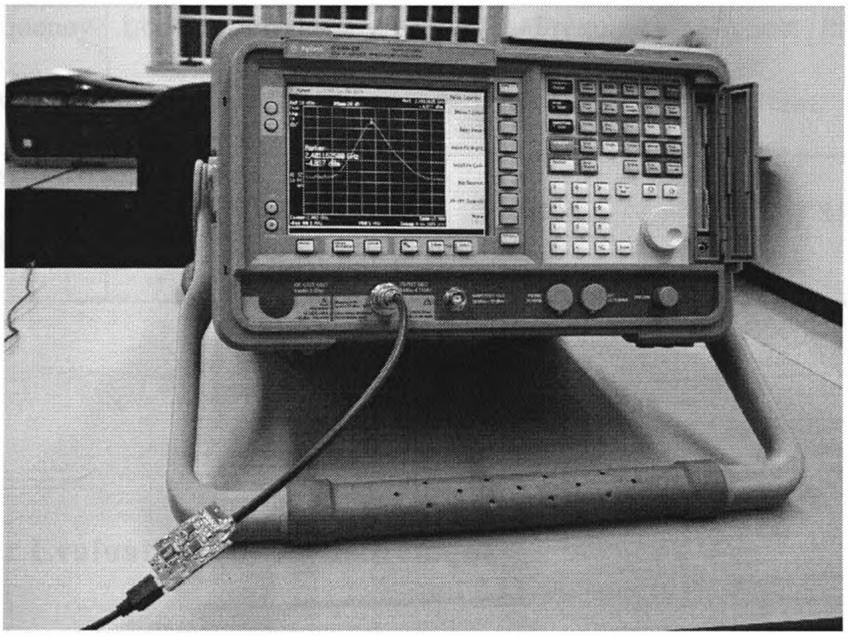

Figure 5-4 Measurement Set-up of Transmitter

5.2.1.2 Measurement Results of Single Channel

Table 5-4 and Table 5-5 show the measurement results of transmitter and receiver.

RF Frequency in Transmitter	Lowest Frequency 2.400Ghz	Middle Frequency 2.464Ghz	Highest Frequency 2.527Ghz
Transmission Power(dBm)	-1.596	-1.094	-2.584

Table 5-4 Transmitter RF Power Results

RF Frequency in Receiver	Lowest Frequency 2.400Ghz	Middle Frequency 2.464Ghz	Highest Frequency 2.527Ghz
Transmission power(dBm)	-1.057	-0.804	-3.814

Table 5-5 Receiver RF Power Results

5.2.2 Kleer Evaluation Kit Measurement

We also measured Kleer evaluation kit RF power as a reference to our design. We set the kit via Kleer development tool as shown in Figure 5-5.

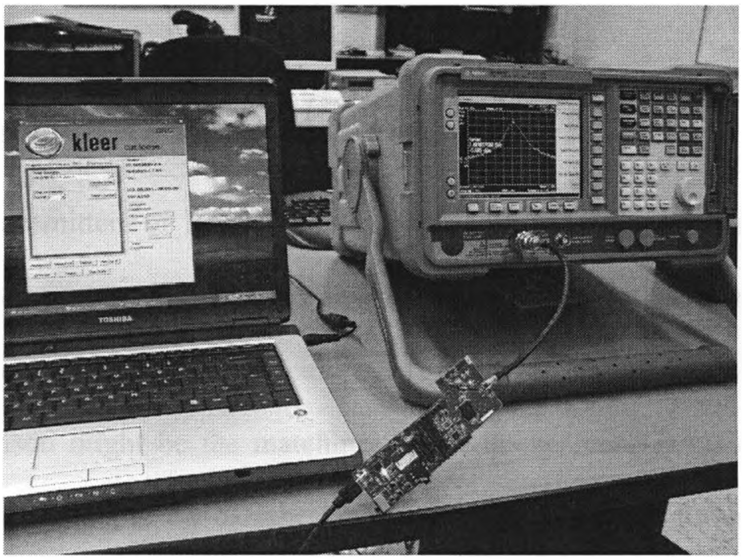

Figure 5-5 Measurement Set-up of Kleer Wireless Audio System

Table 5-6 and Table 5-7 show the measurement results in single channel of Kleer transmitter and receiver.

RF Frequency in Transmitter	Lowest Frequency 2.403Ghz	Middle Frequency 2.438Ghz	Highest Frequency 2.478Ghz
Transmission Power(dBm)	-1.408	-1.574	-0.574

Table 5-6 RF Power of Transmitter of Kleer

RF Frequency in Receiver	Lowest Frequency 2.403Ghz	Middle Frequency 2.438Ghz	Highest Frequency 2.478Ghz
Transmission power(dBm)	-0.694	-0.029	-0.272

Table 5-7 RF Power of Receiver of Kleer

5.2.3 Conclusion of RF Power Measurement

RF power in transmitters of Nordic was around -1dBm. Taking account of the testing cable loss and connection loss, the transmission power is close to that from the data sheet. The transmission power of the receiver of Kleer is higher than Nordic around 0.5dBm.The reason might be the matching circuit in the receiver matched the testing cable better. According to the datasheet, the transmission power in transmitter of Kleer can reach 1.5dBm. The RF power analysis showed that designed wireless system performs comparably to a commercially available wireless audio system.

5.3 Electroacoustic Measurements of the Wired and Wireless System

5.3.1 Wired System Electroacoustic Measurement

Figure 5-6 shows the experimental set-up for the electroacoustic evaluation of the wired system. The output audio from wired system was sent to Sennheiser ER-3A headphone. The output of the microphone was connected to a microphone preamplifier and then goes to a USB-PRE data acquisition system. Spectrum analyzer software running on the laptop was used to analyze the spectrum of the signal from amplifier.

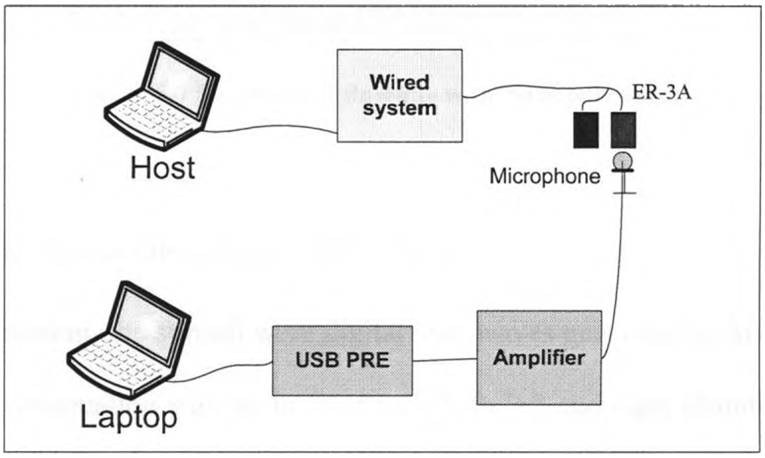

Figure 5-6 Experimental Set-up of Wired System

Firstly, we measured the baseline, no signal playing through the headphones. The result is shown in Figure 5-7, where, apart from the ubiquitous low frequency noise, the noise floor from the system is close to 0 dB SPL.

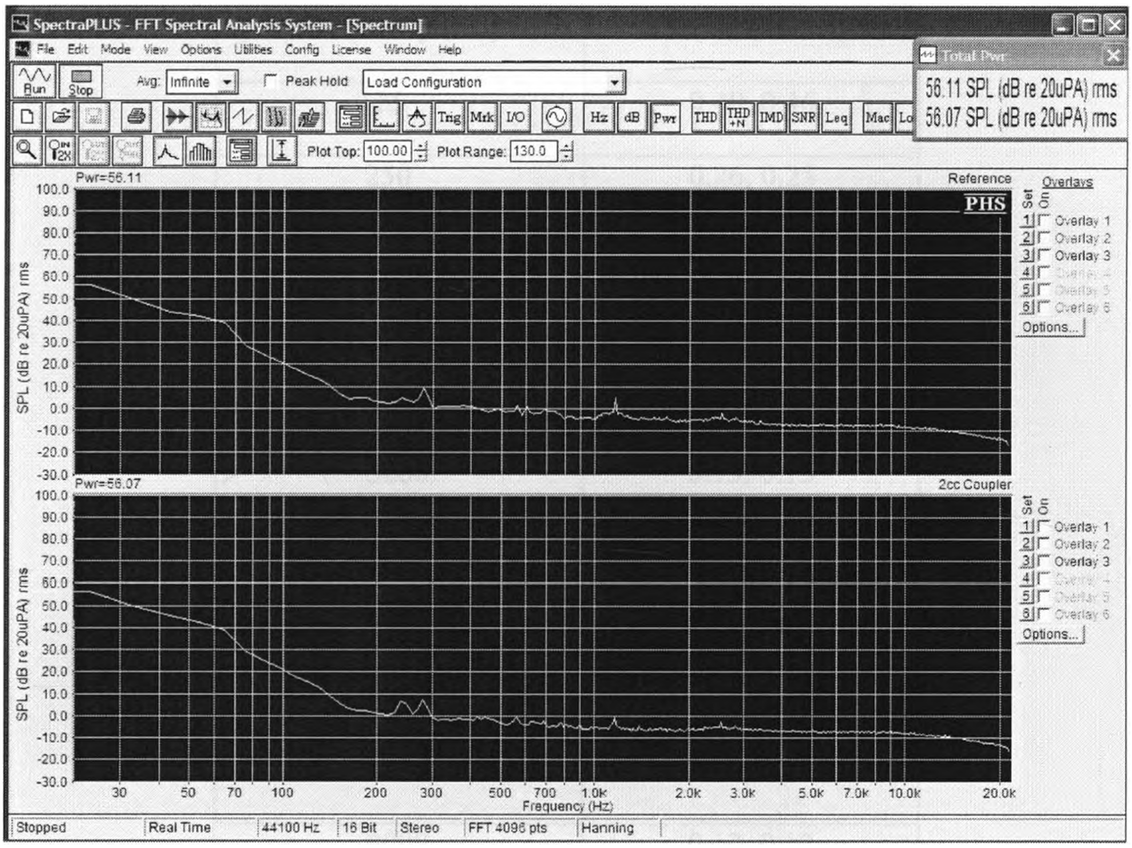

Figure 5-7 Spectrum of Baseline with No Input Signal

5.3.1.1 Total Harmonic Distortion (THD) Measurement

In THD measurement, the stimuli were digital sine waves generated in MATLAB at 90% full scale. The attenuation was set to 20 dB on both left and right channels of the wired system, and the THD values were measured in SpectraPlus at different frequencies. The results are shown in Table 5-8, where the THD values can be seen to be less than 0.5% at all frequencies. This corresponds well with the ANSI S3.6-2004 specification for audiometers that the maximum THD for earphones should be less than 2.5% from 125 to 16,000 Hz [33].

Frequency (Hz)	THD (%) (left, right)
125	0.49, 0.46
250	0.26, 0.25
500	0.37, 0.36
1000	0.20, 0.23
2000	0.54, 0.55
3000	0.13, 0.13
4000	0.06, 0.06
5000	0.05, 0.05
6000	0.10, 0.10
7000	0.10, 0.10
8000	0.12, 0.12

Table 5-8 THD Results of Wired System

5.3.1.2 Sound Pressure Level (SPL) Measurement

Sound pressure level (SPL) is a logarithmic measure of the RMS sound pressure of a sound relative to a reference value. For this experiment, we used a 50 Ω ER-3A transducer [34], another common transducer used in audiometric application, which was connected to the B&K 2 cc coupler and the SpectraPlus signal analysis software. Figure 5-8 reports the SPLs measured at various frequencies, which correspond with the data presented in Frank & Richards [34].

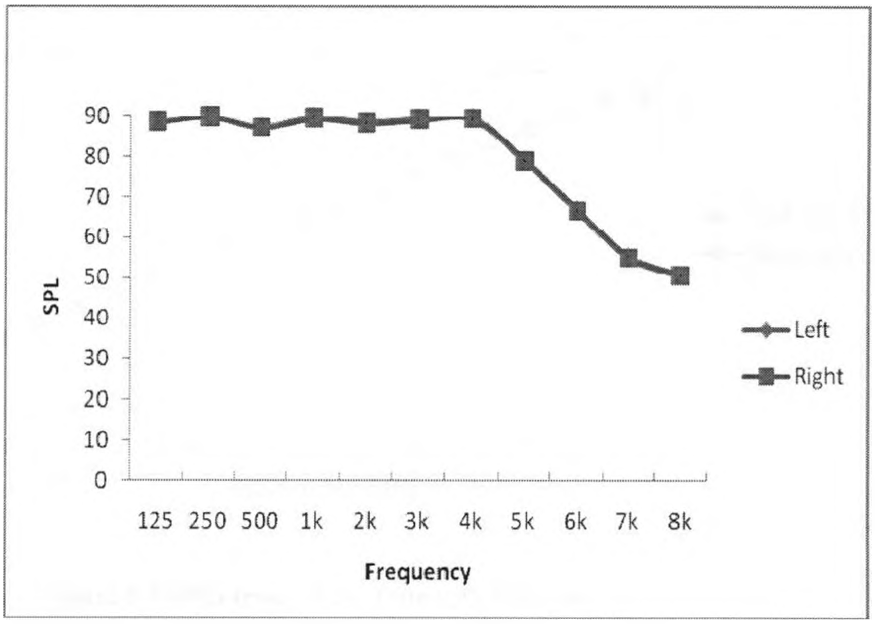

Figure 5-8 SPLs from Wired System in 20dB Attenuation

We also measured the SPLs from 1 kHz, 90% full scale sine wave with different attenuation for calibration and for determining the attenuator linearity. The results are shown in Figure 5-9. However, in 0 dB attenuation, the data were not as expected. The reason might be that the output is too loud and caused some distortion to transducer because the maximum output is around 110db HL [34].

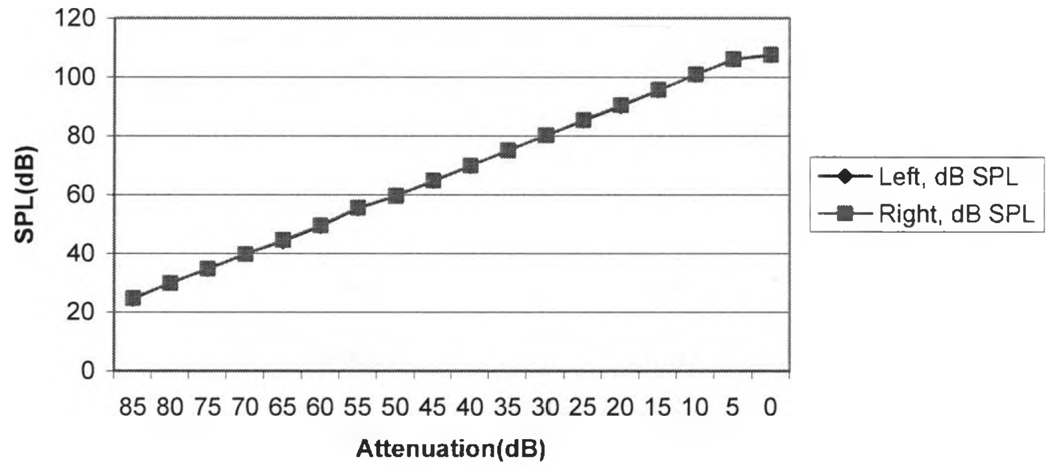

Figure 5-9 SPLs from 1 kHz Tone with Different Attenuation

5.3.2 Wireless System Electroacoustic Measurement

We used the same set-up and steps to measure the wireless system. The only difference was that the headphone was connected to receiver.

5.3.2.1 Total Harmonic Distortion (THD) Measurement of Wireless System

The THD measurements were conducted in a manner similar to those reported for the wired system. Table 5-9 lists the THD values for the left and right channels, which once again can be seen to be less than 0.55%.

Frequency (Hz)	THD (%) (left, right)
125	0.45, 0.43
250	0.24, 0.22
500	0.25, 0.26

1000	0.16, 0.14
2000	0.30, 0.29
3000	0.07, 0.07
4000	0.03, 0.03
5000	0.03, 0.03
6000	0.07, 0.07
7000	0.18, 0.19
8000	0.20, 0.20

Table 5-9 THD Results of Wireless System

It is pertinent to note here that the SPL and attenuator linearity measurements were similar to those reported for the wired system, attesting the transparency of the wireless transmitter/receiver combination.

5.4 Subjective Evaluation

In addition to objective evaluations, the wireless system was evaluated through subjective testing. The administered psychoacoustic tests included frequency discrimination, gap detection and TMTF (temporal modulation transfer function). Figure 5-10 shows the experimental setup for the subjective test. All devices and subject were in the sound booth, while the headphone used was HDA200.

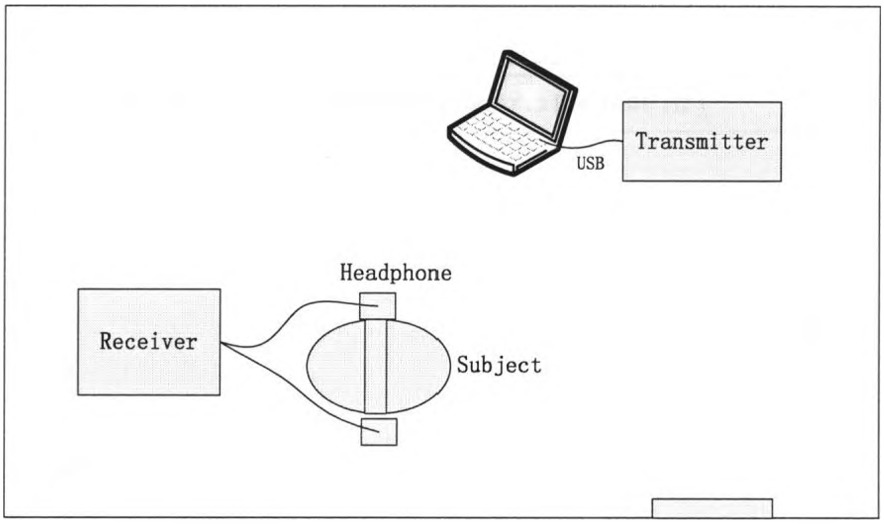

Figure 5-10 Experimental Set-up for Subjective Evaluation

In the frequency discrimination test, the target frequency, signal duration, inter-stimuli interval, initial frequency and SPL can be changed. The application software presents three tones, two of which have the same target frequency while the other one is different. The subject was asked to judge which tone was different from other two tones. If the subject gave the right answer of the test, the difference between the target and the test frequency is reduced, and if the subject answered incorrectly, the difference increased. By using this adaptive procedure, the frequency discrimination threshold at a give target frequency can be obtained. Figure 5-11 displays the tracking procedure used by the software in determining the threshold. Similar adaptive procedure is followed for the gap detection, and TMTF threshold determination. In gap detection test, the initial gap, signal duration, inter-stimuli interval and initial frequency and SPL can be adjusted. In TMTF test, either uniform noise or tone can be chosen as well as carrier frequency. The parameters such as modulation frequency, step size and SPL are adjustable.

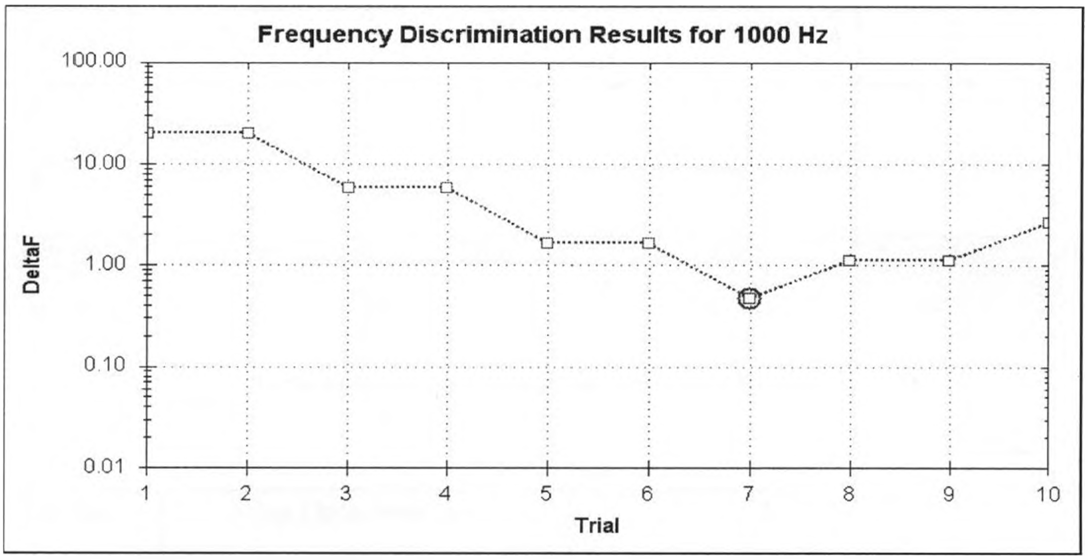

Figure 5-11 Screenshot of Frequency Discrimination Results

Table 5-10 shows the results produced by the wireless system for the frequency discrimination with 9 normal hearing listeners at different frequencies, while the gap detection and TMTF results are displayed in Table 5-12.

Listener	Freq'y Discrimination at 500 Hz (%)	Freq'y Discrimination at 1000 Hz (%)	Freq'y Discrimination at 2000 Hz (%)	Freq'y Discrimination at 4000 Hz (%)
MH	1.08	1.10	0.26	0.41
BL	1.03	1.21	0.53	0.39
JP	0.87	0.35	0.50	1.84
KG	0.70	0.93	0.18	0.47
KA	0.97	8.10	8.54	3.77

TL	0.62	1.47	0.76	0.43
HJ	0.56	0.26	0.60	0.50
NP	10.25	9.55	6.73	0.97
LB	2.40	3.13	9.27	3.57
AVG	2.05	2.90	3.04	1.37

Table 5-10 Frequency Discrimination Test Results

Listener	Gap Detection(ms)	TMTF (dB)
MH	2.90	-24.52
BL	3.21	-23.52
JP	2.86	-27.89
KG	2.87	-24.23
KA	2.68	-18.93
TL	2.87	-22.89
HJ	2.43	-27.27
NP	2.87	-16.02
LB	2.90	-23.02
AVG	2.84	-23.14

Table 5-11 Results of Gap Detection and TMTF

Key observations from this portion of the system evaluation include:

- The normative frequency discrimination thresholds are around 1% across the range of target frequencies [e.g., 35]. The averaged data in Table 5-10 are slightly above this norm, which perhaps is a result of the auditory characteristics of some of the individuals tested. It can be seen from Table 5-10 that for a majority of listeners, the threshold was around 1% across the target frequencies. There are a few listeners (e.g., NP and LB) with supposedly "normal hearing" with elevated frequency discrimination thresholds. This is not uncommon as shown in Figure 5-12. In this Figure, the frequency discrimination data collected from normal hearing listeners using the research-grade TDT based psychoacoustic system, and an earlier version of the wireless prototype is displayed.

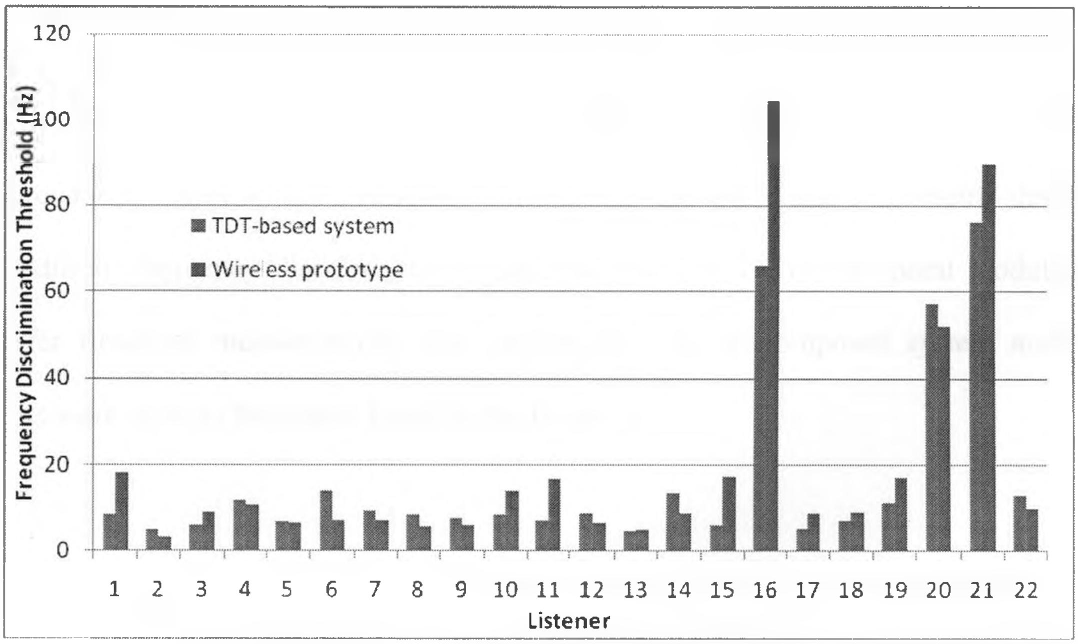

Figure 5-12 Frequency Discrimination Results from the Same Group of Listeners with the TDT and the Wireless Prototype

The y-axis in Figure 5-12 shows the frequency discrimination threshold in Hz for a 1000 Hz target frequency. Again for the majority of listeners, the threshold is around 10 Hz (or 1%). For three listeners, the frequency discrimination was over 40 Hz. Thus, even with presumed normal hearing, elevated frequency discrimination thresholds do occur. Another point worth noting here is that there was no statistically significant difference between the TDT-data and the Wireless-data.

- The normative value for detecting gaps in noise is around 3 – 4 ms [12], and the normative value for the TMTF test is around -20 dB [10]. The results from our evaluation agree with this normative data.

5.5 Summary

The wired and wireless electroacoustic systems were evaluated in this chapter. Both objective and subjective evaluation were undertaken. These measurements revealed that the frequency response and distortion values are in line with other audiometric devices. In addition, frequency discrimination, gap detection and TMTF (temporal modulation transfer function) measurements were performed with the proposed system and the results were close to the norms found in the literature.

Chapter 6

Conclusions

The goal of this project was to design and develop portable testing systems that offer comprehensive evaluations of auditory function. A wired and wireless psychoacoustic testing system were successfully designed, implemented and evaluated. The main features of the proposed system are

- Portability: the wired system attaches to the host through a USB cable and in wireless system, only a tiny transmitter connects to the USB port.
- Versatility: the systems are capable of conducting a number of two channel psychoacoustic tests that comprehensively measure an individual's hearing abilities.
- Flexibility: since the system is controlled through software, it is easy to incorporate custom audiometric testing paradigms.

6.1 Main Contributions

The major contributions of this thesis include:

1. Hardware and firmware implementation of wired and wireless systems – The designed wired system includes a USB audio I/O controller chip for communicating with the software application on the host through a USB cable. The wireless system consists of a transmitter and a receiver. The transmitter is to transmit audio signal to receiver. Both systems are capable of setting audio

signal level and feeding back button status. The firmware for microcontrollers in each system were developed and worked as expected.

2. PCB layout – Due to the size limitation, double-sided PCB boards populated with 0603 SMD parts, 2.4GHz wireless IC and high quality D/A converter was designed and fabricated. EMC was considered since there are analog, digital and 2.4Ghz RF signals in one board.
3. Evaluation of the portable systems – The systems were evaluated with electrical parameters as well as wireless measurement. In addition to these, the entire systems were successfully deployed in sound booth at the National Centre for Audiology and their performances were evaluated through a series of electroacoustic measurements and subjective evaluations.

6.2 Future Work

The wired and wireless systems are point-to-point communication. One tester and one testee mode is supported which can satisfy most hearing evaluations. However, it is promising to test a group of listeners in the same time. Since wireless transmission removes the need of wire connection, it is attractive if one-transmitter and multiple-receiver mode as shown in Figure 6-1 is implemented.

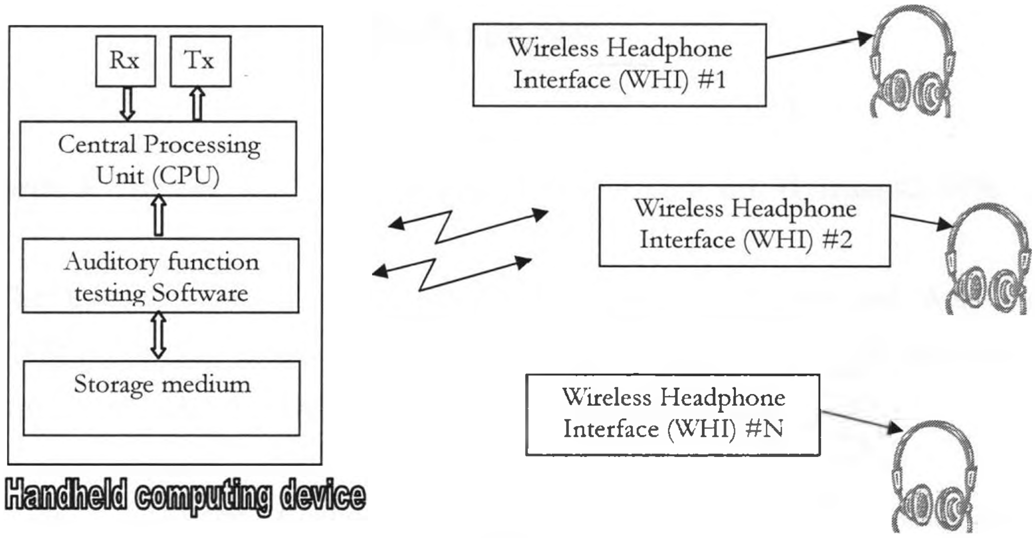

Figure 6-1 One-to-multiple Communication Plan

In addition to the button response function, it is more convenient if the receiver is able to send out voice to transmitter.

As mentioned in previous chapter, the receiver PCB size is 77mmx49mm. The battery is 7.2v Lithium. Compared to the transmitter, the receiver is bigger and heavier. In the future work, these problems could be solved if we use DC/DC converter and 3.6V battery as well as better PCB layout for low noise and high density.

References

[1] Harris, J. "Hearing loss", *Audio-Digest Otolaryngology*, vol. 31, Issue #2, 1998.

[2] The Canadian Association of Speech-Language Pathologists and Audiologists (CASLPA) fact sheet on adult hearing disorders. Available online at http://www.caslpa.ca/PDF/fact%20sheets/adult hearing disorders.pdf

[3] Brian C.J. Moore, *Cochlear Hearing Loss Physiological, Psychological and Technical Issues,* 2nd ed., John Wiley& Son Ltd, 2007.

[4] Chermak, G.D., & Musiek, F.E. *Central auditory processing disorders: New perspectives*. San Diego: Singular Publishing Group, 1997.

[5] Bellis, T.J. & Beck, D.L. "(Central) auditory processing disorders. Overview and amplification issues", *The Hearing Journal,* 60, pp 44 – 47, 2007.

[6] D. S. Dalton, K. J. Cruickshanks, B. E. K. Klein, R. Klein, T. L. Wiley and D. M. Nondahl, "The Impact of Hearing Loss on Quality of Life in Older Adults," *The Gerontologist*, vol. 43, pp. 661-668, 2003.

[7] Newby, H. A. and Popelka, G. R. *Audiology,* 6th ed., Prentice Hall Inc., Englewood Cliffs, New Jersey, 1992.

[8] Moore, D.R. "Auditory processing disorders: Acquisition and treatment", *Journal of Communication Disorders,* 40, 4, pp 295 – 304, 2007.

[9] Moore, David R. "Auditory processing disorder (APD): Definition, diagnosis, neural basis, and intervention", *Audiological Medicine*,4, pp 4 -11, 2006.

[10] Viemeister,N.F. "Temporal modulation transfer functions based upon modulation thresholds," J. Acoust. Soc. Am. 66, 1364-1380, 1979.

[11] Zeng, F-G., Oba, S., Garde, S., Sininger, Y., & Starr, A. "Temporal and speech processing deficits in auditory neuropathy", *Neuroreport,* vol. 10, pp 3429 – 3435, 1999.

[12] Dawes, P., Bishop, D.V.M., Sirimanna, T. & Damiou, D. "Profile and aetiology of children diagnosed with auditory processing disorder (APD)", *International Journal of Pediatric Otorhinolaryngology*, Vol. 72, pp 483-489, 2008.

[13] Jerger, J. & Musiek, F. "Report of the consensus conference on the diagnosis of auditory processing disorders in school-age children", *Journal of the American Academy of Audiology,* vol. 11, pp 467 – 474, 2000.

[14] Catalog of Auditec Inc., Available online at http://www.auditec.com/cgi/auditeccatalog20071212.pdf

[15] Tucker-Davis Technologies Inc., "Introductions of Psychoacoustics & Speech Workstation", Available online at http://www.tdt.com/workstations/Psychoacoustics.htm

[16] John Hyde, *USB Design by Example A Practical Guide to Building I/O Devices.,* John Wiley& Son Ltd, 1999.

[17] Bluetooth SIG Inc., "How Bluetooth Technology Works", Available on line at http://www.bluetooth.com/Bluetooth/Technology/Works/

[18] Free2move AB Corp., *Low power Audio Bluetooth Module with antenna F2M03ALA Datasheet,* 2007.

[19] Kleer Corp., *Kleer Audio LP KLR3012 Preliminary Datasheet.* 2008.

[20] Nordic Semiconductor Corp., *nRF24Z1 headphone reference design, nRF24Z1-HPR1.* January 2006.

[21] Craig Peacock, "USB in a Nutshell", Available on line at http://www.beyondlogic.org/usbnutshell/usb-in-a-nutshell.pdf

[22] C-MEDIA Electronic INC., *CM108 High Integrated USB Audio I/O Controller Datasheet 1.5*, 2004.

[23] Atmel Corp. *ATmega8A Datasheet,* 2007.

[24] Atmel Corp., *ATmega48A Datasheet,* 2007.

[25] National Semiconductor Corp., *Attenuator LM1973 Data Sheet*, March 2001.

[26] Analog Devices Inc., *Rail-to-rail, High Output Current Amplifier AD8397 datasheet*, 2005.

[27] Sennheiser Electronic Corp., "Instruction for use of HDA200 Headphone", Available online at: http://www.sennheiser.com/sennheiser/products.nsf/resources/7749493A3CFE0D10C12574330042FE38/$File/HDA200_bda.pdf

[28] National Semiconductor Corp., *MAX660 Switched Capacitor Voltage Converter Datasheet,* 2002.

[29] Nordic Semiconductor Corp., *2.4 GHz wireless audio streamer nRF24Z1 Datasheet,* March 2001.

[30] Fractus Corp., *Compact Reach Xtend Chip antenna P/N FR05-S1-N-0-102 Datasheet*, 2007.

[31] Cirrus Logic Semiconductor Corp., *120dB, 192 kHz Multi-Bit DAC with Volume Control CS4398 Datasheet*, July 2005.

[32] National Semiconductor Corp., *LM3480 100mA, SOT23, Quasi Low_Dropout Linear Voltage Regulator Datasheet*, July 2000.

[33] Ross Roeser, Michael Valente, Holly Hosford-Dunn, *Audiology Diagnosis,* 2nd ed. Thieme Medical Publishers, 2007.

[34] Frank T, Richards WD. "Hearing Aid Coupler Output Level Variability and Coupler Correction Levels for Insert Earphones", Ear and Hearing, Vol 12, No.3, 1991.

[35] McDermott, H.J., Lech, M., Kornblum, M.S., Irvine, D.R.F. "Loudness perception and frequency discrimination in subjects with steeply sloping hearing loss: Possible correlates of neural plasticity", Journal *of the Acoustical Society of America,* vol. 104, pp 2314 – 2325, 1998.

Appendix

Ethics Approval Form

Office of Research Ethics

The University of Western Ontario
Room 4180 Support Services Building, London, ON, Canada N6A 5C1
Telephone: (519) 661-3036 Fax: (519) 850-2466 Email: ethics@uwo.ca
Website: www.uwo.ca/research/ethics

Western

Use of Human Subjects - Ethics Approval Notice

Principal Investigator: Dr. V. Parsa
Review Number: 15710E **Review Level:** Expedited
Review Date: December 03, 2008
Protocol Title: Investigation of a hybrid psychoacoustic test platform for use in a clinical setting
Department and Institution: Health & Rehabilitation Sciences, University of Western Ontario
Sponsor: NSERC Idea to Innovation Grant
Ethics Approval Date: February 05, 2009 **Expiry Date:** December 31, 2009
Documents Reviewed and Approved: UWO Protocol, Letter of Information and Consent
Documents Received for Information:

This is to notify you that The University of Western Ontario Research Ethics Board for Health Sciences Research Involving Human Subjects (HSREB) which is organized and operates according to the Tri-Council Policy Statement: Ethical Conduct of Research Involving Humans and the Health Canada/ICH Good Clinical Practice Practices: Consolidated Guidelines; and the applicable laws and regulations of Ontario has reviewed and granted approval to the above referenced study on the approval date noted above. The membership of this REB also complies with the membership requirements for REB's as defined in Division 5 of the Food and Drug Regulations.

The ethics approval for this study shall remain valid until the expiry date noted above assuming timely and acceptable responses to the HSREB's *periodic requests for surveillance and monitoring information.* If you require an updated approval notice prior to that time you must request it using the UWO Updated Approval Request Form.

During the course of the research, no deviations from, or changes to, the protocol or consent form may be initiated without prior written approval from the HSREB except when necessary to eliminate immediate hazards to the subject or when the change(s) involve only logistical or administrative aspects of the study (e.g. change of monitor, telephone number). Expedited review of minor change(s) in ongoing studies will be considered. Subjects must receive a copy of the signed information/consent documentation.

Investigators must promptly also report to the HSREB:

a) changes increasing the risk to the participant(s) and/or affecting significantly the conduct of the study;
b) all adverse and unexpected experiences or events that are both serious and unexpected;
c) new information that may adversely affect the safety of the subjects or the conduct of the study.

If these changes/adverse events require a change to the information/consent documentation, and/or recruitment advertisement, the newly revised information/consent documentation, and/or advertisement, must be submitted to this office for approval.

Members of the HSREB who are named as investigators in research studies, or declare a conflict of interest, do not participate in discussion related to, nor vote on, such studies when they are presented to the HSREB.

Chair of HSREB: Dr. Joseph Gilbert

Ethics Officer to Contact for Further Information

☐ Janice Sutherland	☐ Elizabeth Wambolt	☑ Grace Kelly	☐ Denise Grafton

This is an official document. Please retain the original in your files.

cc: ORE File